

Multi-stage tomography based on eigenanalysis for high-dimensional dense unitary processes in gate-based quantum computers

YANNICK DEVILLE¹, (Member, IEEE), and ALAIN DEVILLE²

¹Université de Toulouse, UPS, CNRS, CNES, OMP, IRAP (Institut de Recherche en Astrophysique et Planétologie), F-31400 Toulouse, France (email: yannick.deville@irap.omp.eu)

²Aix-Marseille Université, CNRS, IM2NP UMR 7334, F-13397 Marseille, France (email: alain.deville@univ-amu.fr)

Corresponding author: Yannick Deville (email: yannick.deville@irap.omp.eu).

ABSTRACT Quantum Process Tomography (QPT) methods aim at identifying, i.e. estimating, a quantum process. QPT is a major quantum information processing tool, since it especially allows one to experimentally characterize the actual behavior of quantum gates, that may be used as the building blocks of quantum computers. We here consider unitary, possibly dense (i.e. without sparsity constraints) processes, which corresponds to isolated systems. Moreover, we develop QPT methods that are applicable to a significant number of qubits and hence to a high state space dimension, which allows one to tackle more complex problems. Using the unitarity of the process allows us to develop methods that first achieve part of QPT by performing an eigenanalysis of the estimated density matrix of a process output. Building upon this idea, we first develop a class of complete algorithms that are single-stage, in the sense that they use only one eigendecomposition. We then extend them to multiple-stage algorithms (i.e. with several eigendecompositions), in order to address high-dimensional state spaces while being less limited by the estimation errors made when using an arbitrary given Quantum State Tomography (QST) algorithm as a building block of our overall methods. We first propose two-stage methods and we then extend them to dichotomic methods, whose number of stages increases with the considered state space dimension. The relevance of our methods is validated with simulations. Single-stage and two-stage methods efficiently apply up to 13 qubits on a standard PC (with 16 GB of RAM). Multi-stage methods yield an even higher accuracy (Normalized Mean Square Error down to 10^{-3}).

INDEX TERMS eigenanalysis of density matrix, high-dimensional quantum state space, quantum computing, quantum gate characterization, quantum machine learning (supervised / semi-supervised / unsupervised), quantum process tomography, quantum state tomography, unitary quantum gate

I. INTRODUCTION

Quantum process tomography (QPT) may be considered as the quantum counterpart of classical system identification [1], that is, system parameter estimation. It was mainly¹ introduced in 1997 in [2] and then extended (together with quantum process learning) e.g. in [1], [3]–[27]. QPT is a major quantum data processing tool, since it especially allows one to characterize the actual behavior of quantum gates, that may be used as the building blocks of quantum computers. This gate-based (or circuit-based) approach builds upon the unitary transforms performed by quantum gates (see Chapter

4 of [1]). It is currently one of the most prominent quantum computing paradigms and various commercial products based on this paradigm are available. This e.g. includes IBM’s Qiskit environment (see [28]–[30] and especially [31] for the use of reversible unitary gates), Amazon’s Braket tool (see [32] especially for reversible transformations), and Mathworks’s software package (see [33] e.g. for their statement “Quantum gates represent reversible operations that transform the quantum state according to unitary matrices”). Due to the importance of the above-mentioned *unitary* processes, various methods dedicated to such processes have been proposed, for performing unitary quantum process esti-

¹See also [1] p. 398 for the other earliest references.

mation/learning (see e.g. [3], [13], [22]–[27]) and e.g. for the related topic of the inversion and transposition of unknown unitary operations [34].

QPT is a ““data-driven”” approach, and can thus be considered as a type of quantum machine learning (QML) problem (see [35] for a taxonomy of QML problems), because the input-output transform performed by the considered process is generally inferred from the values of input quantum states and/or from measurement results for output quantum states of that process. More precisely, usual QPT methods require one to fix *a priori* and hence know the above input ““values”” (i.e. states) of the process and to use information about the corresponding output ““values”” (i.e. states), that is derived from measurements performed at the output of the considered process. This corresponds to the supervised version of machine learning, also called the non-blind version of machine learning [36]. In contrast, the other extreme case is the one which requires the most limited knowledge about the process input whereas output measurements are still used, and this corresponds to the unsupervised, or blind, QPT (BQPT) configuration [36]. BQPT methods were introduced in [37] and then especially developed in [36], [38], [39]. In that case, the individual input state values are completely unknown, that is, neither fixed *a priori* nor estimated by means of measurements: in [37], [38], the input consists of unknown unentangled deterministic-coefficients pure states (DCPS); in [36], [39], it consists of random-coefficient pure states (RCPS) and the information available about these RCPS is restricted to some of their global, i.e. statistical, properties. DCPS are the usual form of pure states of quantum physics, whereas RCPS were introduced in [40] and then discussed in various related papers, especially including [41].

Between the above two extreme cases, a recently introduced approach (see [22] and references therein) was claimed to be semi-blind (i.e. semi-supervised), because it does not require the values of the input quantum states to be fixed *a priori*, but it estimates them, by also performing measurements at the input of the process for part of the available copies of these input states. This method thus allows one to use almost any values for the input states, whereas various supervised QPT methods are more constraining because they are only applicable to a specific, predefined, set of input values.

As detailed below, the different parts and variants of the QPT algorithms proposed in the present paper cover all above three types of learning. Some of them require their input states to be known, so that these states may be fixed *a priori* (supervised learning) or estimated from measurements (semi-supervised learning). Other parts and variants of our algorithms use input states whose values are not known, but that are required to meet a given condition (unsupervised learning). Besides, part of the proposed algorithms use ““pure states””, where we employ the term ““pure states”” in the above-defined usual sense, that is, DCPS. In contrast, other proposed algorithms use statistical mixtures.

Within the above framework, we focus on an original

case which combines the following two features. First, the considered process is constrained to be unitary, which corresponds to addressing a system that is isolated from its environment. Second, we are mainly interested in the case when the process has a high dimension, because it involves a significant number of qubits. This allows one to tackle more complex problems. We stress that we do not set any other conditions on the considered process. In particular, we allow (but do not request) the matrix that represents that process in the considered basis to be a so-called dense, i.e. non-sparse, matrix (we here use the standard terminology: a sparse matrix is a matrix that has a large percentage of zeros; see e.g. [42]). In contrast, some approaches from the literature for QPT and the related topic of Hamiltonian estimation request sparsity (see e.g. [12], [43]), but this was considered to be less relevant than unitarity in [22] and we explained above when the unitarity assumption is relevant.

Concerning the ““mathematical principles”” of the proposed QPT methods, in this paper we show that one of the key ingredients of our approach is the eigendecomposition of the (estimated) density matrix of a mixed output state of the considered process. Before moving to technical details and a variety of required extensions of this idea in the subsequent sections, this major idea can here be outlined as follows. The first output density matrix of the considered process is here denoted as ρ_2 . As discussed in Section II, this density matrix reads

$$\rho_2 = U \rho_1 U^\dagger \quad (1)$$

where U is the unitary matrix that represents the process to be estimated in the considered basis, $.\dagger$ is the transconjugate (i.e. Hermitian transpose) and ρ_1 is the density matrix of the first input mixed state that yields the output state ρ_2 . The idea is then that, when the density matrix ρ_1 is selected to be diagonal in the considered and fixed basis (computational basis), Eq. (1) is an eigendecomposition of ρ_2 . Therefore, in practice, starting from an estimate of ρ_2 derived from measurements, its eigendecomposition may be hoped to yield a result directly related to an estimate of U . This idea will then have to be refined further in this paper because: 1) eigendecomposition yields indeterminacies (defined below) and 2) fluctuations in output density matrix estimation limit the performance of this preliminary approach and then lead us to extend it in this paper.

The above preliminary description shows that the type of approaches proposed in this paper has some connections with works that were previously reported both in the classical and quantum domains. The connections with classical approaches are discussed in Appendix A, whereas those with the quantum domain may be defined as follows. A few recent papers dealing with quantum data also consider (1) in the framework of QPT. However, they only have the following limited relationships with our investigation. Ref. [44] aims at deriving the number (and values) of quantum states that should be applied to the input of a quantum process to be able to identify that process. However, that paper does not focus

on the same input values as in the present paper and, as also noted in [22], it does not provide an explicit QPT algorithm. Ref. [3] provides such algorithms, that are different from ours and that are tested only for a Hilbert space dimension $d = 5$, whereas we consider dimensions up to $d = 2^{13} \simeq 8000$.

QPT algorithms may also be split in two classes, from the following point of view. Part of them first use the results of measurements at the output of the system by explicitly performing quantum state tomography (QST). This means that they estimate the ket (for a pure state) or the density matrix (for a statistical mixture) that represents that output state. They then use these estimated output states (and the corresponding input states, their estimates or their properties) so as to infer the considered process. Other QPT methods instead directly use the results of the considered types of measurements. In the present paper, we consider the first class of QPT methods and we focus on the part dedicated to QPT itself, as opposed to QST, as detailed in Section V.

The remainder of this paper is organized as follows. Section II is devoted to the introduction of several variants of our basic type of QPT methods, that is, single-stage methods. These methods have a limitation, that is defined in Section III. Therefore, we first introduce the two-stage extensions of the above methods in Section III, and then their general multi-stage form in Section IV. Numerical results illustrate the performance of the proposed methods in Section V and conclusions are drawn from this investigation in Section VI.

II. PROPOSED SINGLE-STAGE QPT METHODS

As stated above, in all the configurations considered in this paper, the quantum system is assumed to be isolated from its environment (the proposed approaches may therefore also be used as an approximation for systems that have a limited interaction with their environment and that therefore lead to near-unitary processes, as in [3]). It is well-known that, in that case, the temporal evolution of the state of that system between given initial and final times is governed by a unitary operator (see [1], [45]; see also [46], [47] for the relationship with the system's Hamiltonian). More precisely, using the above-defined notations, we consider a (first) mixed state defined by a density matrix ρ_1 at an initial time. As explained e.g. in [1], [45], the state of that system at a subsequent, final, time is then defined by a density matrix ρ_2 that may be expressed as in (1), where U is a unitary matrix, that depends on the dynamics of the considered system.

The algorithms proposed in this section to estimate U then consist of two parts. Each part involves a given type of input quantum state and an algorithm for exploiting the associated output quantum state (and possibly the input state). Each of the following subsections describes one of these two parts.

A. FIRST PART OF THE METHODS

We here consider the situation when the first state applied to the analyzed process is a given statistical mixture, represented by the density matrix ρ_1 . The process output is then also a mixed state and its density matrix ρ_2 may be expressed

as (1). More specifically, we here introduce a first variant, in which the matrix ρ_1 is diagonal (see Appendix B about how to create it), whereas Appendix G addresses the more general case when this constraint is removed.

The matrix ρ_2 is known to be Hermitian, since it is a density matrix (see e.g. [45] p. 283). Therefore, it is normal (see [48] p. 100; ²) and hence unitarily diagonalizable: see Theorem 1 and comments in its proof (all theorems cited in the core of this paper are provided in Appendix F). The first part of the QPT method proposed below is based on the eigendecomposition of ρ_2 (because (1) is such an eigendecomposition, as detailed below). More precisely, in practice, what is initially available for performing an eigendecomposition is not the theoretical matrix ρ_2 but an estimate $\hat{\rho}_2$ of ρ_2 , provided by a QST algorithm (we here use standard notations, e.g. as in [50]–[52]: an estimate of an unknown, deterministic, scalar, vector or matrix θ is denoted as $\hat{\theta}$). Therefore, our QPT method preferably starts with two preprocessing steps, that consist of first deriving a Hermitian estimate $\hat{\rho}_3$ from $\hat{\rho}_2$ and then a unit-trace estimate $\hat{\rho}_4$ from $\hat{\rho}_3$ (see details in Appendix C), unless the considered QST algorithm already guarantees that $\hat{\rho}_2$ meets these two properties.

Then, the core of our QPT algorithm performs an eigendecomposition of the Hermitian matrix $\hat{\rho}_4$. This eigendecomposition problem has several solutions, corresponding to the indeterminacies of eigendecomposition detailed below. Any of these solutions is defined by two matrices, hereafter denoted as D_4 and V_4 . D_4 is a diagonal matrix that contains the eigenvalues of $\hat{\rho}_4$ in an arbitrary order (see e.g. [48] p. 102). Moreover, each column of V_4 is an eigenvector of $\hat{\rho}_4$ (see (2) and Theorem 2) and V_4 is here unitary (because $\hat{\rho}_4$ is unitarily diagonalizable), hence $V_4^{-1} = V_4^\dagger$. These results V_4 and D_4 of the eigendecomposition are linked to the initial matrix $\hat{\rho}_4$ as follows:

$$\hat{\rho}_4 = V_4 D_4 V_4^{-1} \quad (2)$$

$$= V_4 D_4 V_4^\dagger. \quad (3)$$

Comparing (3) to (1), with $\hat{\rho}_4$ an estimate of ρ_2 and with ρ_1 a diagonal matrix, shows that (1) is one of the possible eigendecompositions of $\hat{\rho}_4$ up to estimation errors. Therefore, the matrices D_4 and V_4 obtained in practice with our algorithm are respectively equal to ρ_1 and U up to the indeterminacies of the eigendecomposition process (and up to estimation errors). In particular, V_4 is the first obtained quantity related to the estimation of U (it could therefore be denoted as \hat{U}_1). We now define its indeterminacies in more detail, and we show how to solve them.

In our first type of QPT methods described here, we constrain all diagonal values of the user-defined matrix ρ_1 to be different. This means that all eigenvalues in the eigendecompositions of ρ_2 and hence $\hat{\rho}_4$ (ignoring estimation errors) are different. Therefore, each of them is associated with a different one-dimensional eigenspace. In other words,

²Throughout this paper, the reader may refer to [49], instead of [48].

all eigenvectors corresponding to a given eigenvalue are along the same direction and the directions associated with two different eigenvalues are different (this is true for any complex square matrix: see [48] p. 47) and even orthogonal: see Theorem 3. Each eigenvalue is thus coupled with a single eigenvector in any considered eigendecomposition. The first indeterminacy of the eigendecomposition of $\hat{\rho}_4$ is then a possible *coupled* permutation of 1) the columns of the matrix V_4 obtained as a first quantity towards the estimation of U in this eigendecomposition and 2) the values along the diagonal of the matrix D_4 , due to the above-mentioned arbitrary order of the latter diagonal values. This permutation problem may be solved as follows. As stated above, we constrain all diagonal values of ρ_1 to be different (at this stage of the discussion, we restrict ourselves to a theoretical approach, where we only need the eigenvalues to be different; further in this paper, we will discuss the gap required between them, when considering practical implementations of our approach: see Appendix D for the method considered in the present section). Moreover, we constrain all diagonal values of ρ_1 to be placed on that diagonal according to a given order. Hereafter, we will consider the case when they are in decreasing order. With respect to the above-defined machine learning terminology, this part of our algorithm is thus unsupervised: it does not require the exact value of the input state, i.e. the input density matrix ρ_1 , to be known but it sets limited conditions on some of its properties.

The above known order of the diagonal values of ρ_1 is used to postprocess D_4 , by permuting the values obtained on its diagonal so that they are in the same order as the order that we impose on ρ_1 . More precisely, in the case considered hereafter, we permute the values obtained on the diagonal of D_4 so that they are in decreasing order (if some eigenvalues obtained in practice are nonreal, they are ordered according to their moduli). Since we now know which permutation is required to this end, we then use that specific permutation to reorder the columns of V_4 in the same way. The matrix with reordered columns thus obtained is denoted as \hat{U}_2 , since it is the second quantity that we build for estimating U .

Thanks to the above approach, the only indeterminacy that remains in \hat{U}_2 with respect to U is an unknown complex scale factor in each of its columns, since any such column belongs to the adequate one-dimensional eigenspace and is therefore defined up to a complex scale factor. Moreover, we create \hat{U}_2 so that each of its columns has unit norm. To this end, if the considered eigendecomposition algorithm does not directly guarantee that this unit-norm condition is met, we postprocess the value of \hat{U}_2 that it yields, by dividing each column of \hat{U}_2 by its norm. After this postprocessing, the scale factor of each column of \hat{U}_2 , with respect to the column of U that has the same index, reduces to a unit-modulus factor, i.e. a phase factor, because U is unitary and therefore all its columns have unit norm, as those of \hat{U}_2 . \hat{U}_2 then reads

$$\hat{U}_2 = [e^{i\phi_1} u_1, \dots, e^{i\phi_d} u_d] \quad (4)$$

where u_1, \dots, u_d are the column vectors of the actual matrix

U and ϕ_1, \dots, ϕ_d are the phase indeterminacies with respect to the above vectors that remain at this stage. Denoting D_ϕ the diagonal matrix that contains the unknown phase factors $e^{i\phi_1}, \dots, e^{i\phi_d}$ on its main diagonal, (4) reads

$$\hat{U}_2 = U D_\phi. \quad (5)$$

The second part of our algorithm, presented below in Section II-B, aims at determining all phase factors $e^{i\phi_1}, \dots, e^{i\phi_d}$, up to a global phase factor (a process matrix U can only be defined up to a single, i.e. global, phase factor).

B. SECOND PART OF THE METHODS

Thanks to the limited number of unknowns (namely the phase factors $e^{i\phi_1}, \dots, e^{i\phi_d}$) that remain in the matrix \hat{U}_2 of (4) obtained in Section II-A, a single and pure state is then sufficient for estimating these unknowns. This yields the first variant of the second part of our methods, presented here. However, one may instead use a mixed state for estimating these unknowns, as shown in Appendix H.

We therefore here apply a known pure state, defined by a ket $|\Psi_1\rangle$, at the input of the process (this part of the algorithm is therefore supervised, or semi-supervised if $|\Psi_1\rangle$ is initially unknown but estimated by performing measurements for part of the available copies of that state; for the supervised case, Appendix E explains how $|\Psi_1\rangle$ is chosen). The corresponding pure state at the output of that process is defined by the ket

$$|\Psi_2\rangle = U|\Psi_1\rangle. \quad (6)$$

What is available in practice is a ket $|\hat{\Psi}_2\rangle$, obtained by performing a QST at the output of the process, and equal to $|\Psi_2\rangle$ up to an unknown phase factor and to estimation errors (see again Appendix C concerning a possible normalization of the QST output used here). When neglecting the above estimation errors,

$$|\hat{\Psi}_2\rangle = e^{i\theta}|\Psi_2\rangle \quad (7)$$

$$= e^{i\theta}U|\Psi_1\rangle. \quad (8)$$

Our algorithm computes the ket

$$|\Psi_3\rangle = \hat{U}_2^\dagger|\hat{\Psi}_2\rangle, \quad (9)$$

based on the following motivation: combining (9), (5), (8) and considering that U is unitary (hence $U^\dagger U = I$) yields

$$|\Psi_3\rangle = e^{i\theta}D_\phi^*|\Psi_1\rangle \quad (10)$$

where $*$ stands for conjugation. This equation is very useful because, apart from the global phase θ , its only unknown is D_ϕ , i.e. the set of phase factors $e^{i\phi_1}, \dots, e^{i\phi_d}$ to be determined. This problem is easily solved by considering each component k , denoted as $|\cdot\rangle_k$, of the above kets. Using a ket $|\Psi_1\rangle$ with nonzero components, (10) yields

$$\frac{|\Psi_3\rangle_k}{|\Psi_1\rangle_k} = e^{i(\theta-\phi_k)} \quad \forall k \in \{1, \dots, d\}. \quad (11)$$

The associated matrix form reads

$$\text{diag}(|\Psi_3\rangle \otimes |\Psi_1\rangle) = e^{i\theta}D_\phi^* \quad (12)$$

Input : a) Estimate $\hat{\rho}_4$ of output density matrix ρ_2 (provided by Quantum State Tomography (QST) and obtained for input density matrix (40)). b) Estimate $|\hat{\Psi}_2\rangle$ of output ket $|\Psi_2\rangle$ (provided by QST and obtained for all components of input ket $|\Psi_1\rangle$ equal to $1/\sqrt{d}$).

Output: Estimate \hat{U}_5 of quantum process matrix U .

begin

```

/* Exploit  $\hat{\rho}_4$ : */  

Eigendecomposition: derive 1) a diagonal matrix  

 $D_4$  that contains the eigenvalues of  $\hat{\rho}_4$  in an  

arbitrary order and 2) a matrix  $V_4$  whose  

columns are eigenvectors of  $\hat{\rho}_4$  in the same order  

as eigenvalues;  

Reorder the eigenvalues in  $D_4$  in decreasing order  

and apply the same permutation to the columns  

of  $V_4$  to create the matrix  $\hat{U}_2$ ;  

/* If the above  

eigendecomposition algorithm  

does not yield unit-norm  

eigenvectors, then create them  

as follows: */  

Divide each column of  $\hat{U}_2$  by its norm;  

/* Exploit  $|\hat{\Psi}_2\rangle$ : */  

 $|\Psi_3\rangle = \hat{U}_2^\dagger |\hat{\Psi}_2\rangle$ ;  

 $\hat{U}_5 = \hat{U}_2 \text{diag}(|\Psi_3\rangle \oslash |\Psi_1\rangle)$ ;
```

end

Algorithm 1: EQPT1: first Eigenanalysis-based Quantum Process Tomography algorithm (composed of one stage). This version is for the case when the QST algorithm provides estimates that meet the known properties of the actual quantities. Otherwise, see Appendix C.

where \oslash is the element-wise division for vectors (as defined in Appendix F) and $\text{diag}(v)$ is the diagonal matrix that contains all elements of a vector v on its main diagonal.

Based on the above properties, the final step of our algorithm creates, as follows, a new estimate of U denoted as \hat{U}_5 (the intermediate notations \hat{U}_3 and \hat{U}_4 are not used here but are required for the two-stage methods of Section III):

$$\hat{U}_5 = \hat{U}_2 \text{diag}(|\Psi_3\rangle \oslash |\Psi_1\rangle). \quad (13)$$

This approach is used because, due to (12) and (5), Eq. (13) yields

$$\hat{U}_5 = e^{i\theta} U \quad (14)$$

which means that \hat{U}_5 succeeds in restoring U , up to a global phase factor (and again up to the estimation errors that were mentioned above but implicit in the above equations).

A pseudo-code of the version of our algorithm corresponding to all this Section II is provided in Algorithm 1. This algorithm is called EQPT1, because it is our first proposed Eigenanalysis-based QPT algorithm.

III. PROPOSED TWO-STAGE QPT METHODS

A. MOTIVATION

The dimension d of the state space (and hence the dimension $d \times d$ of the considered process matrix U) that can be addressed by the type of QPT methods proposed in Section II is limited by the following phenomenon. As explained in that section, these methods require all eigenvalues of the input density matrix ρ_1 of the process to be different. Moreover, they should be separated by a minimum gap to be distinguishable, so that their estimates are not permuted in practice (in order to reorder them and the associated eigenvectors correctly). Besides, all of them range from 0 to 1, because they are nonnegative and their sum is equal to one, as stated above. All these conditions yield an upper bound, denoted as n_{max} , for the acceptable number of eigenvalues of ρ_1 . Since the number of (different) eigenvalues of ρ_1 is always equal to d for the methods of Section II, this yields an upper bound for the state space dimension d that can be handled by these methods, and this bound on d is also equal to n_{max} :

$$d \leq n_{max}. \quad (15)$$

In the present section, we aim at addressing higher values of d . To this end, we move to the case when some eigenvalues of the input density matrix ρ_1 are equal and we therefore introduce extensions of the QPT methods of Section II to be able to handle that more complex case.

B. FIRST PART OF THE METHODS

As in Section II-A, the method proposed here starts by considering a given mixed state that has a diagonal density matrix ρ_1 and that is applied to the input of the considered unitary process defined by a matrix U . However, we here accept to have identical values on the main diagonal of ρ_1 , at the expense of then having to handle more complex eigen-decomposition properties for the process output, as shown below. More precisely, each value that appears on the main diagonal of ρ_1 appears d_1 times, on adjacent rows, and that diagonal contains d_2 different values. The number of rows of ρ_1 , equal to the dimension of the considered state space, is thus equal to

$$d = d_1 d_2 \quad (16)$$

(in practice, we aim at considering the case when d_1 , d_2 , and hence d are powers of 2, with an application to qubits). If requesting the same minimum gap between different eigenvalues as in Section II-A, or in other words, if replacing the bound (15) on d in Section II by the same bound value for d_2 instead of d here, then the maximum value of the state space dimension (16) that can be handled here is d_1 times higher than the maximum dimension that can be addressed by the methods of Section II, which is our goal, ideally. However, it is not guaranteed that the methods proposed hereafter can handle the same gap between different eigenvalues as in Section II-A with the same accuracy, especially due to the more complex structure of these extended methods. The practical

accuracy of all proposed methods is therefore investigated numerically further in this paper.

Denoting r_1, \dots, r_{d_2} the different eigenvalues of ρ_1 , that chosen density matrix reads

$$\rho_1 = \begin{bmatrix} r_1 & 0 & \dots & & 0 \\ & \ddots & & & \\ & & r_1 & & \\ & & & r_2 & \\ & & & & \ddots \\ & 0 & \dots & & 0 & r_{d_2} \end{bmatrix} \quad (17)$$

with each diagonal value repeated d_1 times. This may also be expressed as

$$\rho_1 = \text{diag}(r) \otimes I_{d_1} \quad (18)$$

where r is the vector that contains the values r_1, \dots, r_{d_2} , whereas I_{d_1} is the $d_1 \times d_1$ identity matrix and \otimes stands for the Kronecker product [53]. Without loss of generality, we here again request the values on the diagonal of ρ_1 to be in nonincreasing order: $r_1 > r_2 > \dots > r_{d_2}$. Moreover, we preferably use values that are uniformly distributed (that is, multiples of the same step, with zero excluded), as in the method of Section II (see details for the latter method in Appendix D). In the configuration of the present section, (40) is thus replaced by:

$$r_k = \frac{2(d_2 - k + 1)}{d(d_2 + 1)} \quad k \in \{1, \dots, d_2\}. \quad (19)$$

Here again, the process output corresponding to ρ_1 is a mixed state and its density matrix ρ_2 may be expressed as (1). Moreover, as in Section II-A, ρ_2 is Hermitian and hence unitarily diagonalizable, and it has unit trace. Besides, in practice, an estimate $\hat{\rho}_2$ of ρ_2 is derived by a QST algorithm and, if required by the considered QST algorithm, we preprocess this estimate of ρ_2 in order to derive its Hermitian and unit-trace version, denoted as $\hat{\rho}_4$. We then perform an eigendecomposition of $\hat{\rho}_4$. The analysis of the properties of this eigendecomposition here requires additional care, because the considered matrix has various *identical* eigenvalues.

The properties of Section II-A that remain true here are as follows. The eigendecomposition is not unique, Eq. (2)-(3) still apply, V_4 and D_4 are respectively a unitary matrix and a diagonal matrix, the k th column of V_4 is an eigenvector of $\hat{\rho}_4$ and the associated eigenvalue is the k th value on the diagonal of D_4 (see again Theorem 2 for the latter property).

In contrast, what is different here as compared with Section II-A is that the same eigenvalue here appears d_1 time and is thus associated with d_1 eigenvectors, instead of only one in Section II-A. Eigendecomposition properties are more complex than above in this general framework but, fortunately, their complexity is here limited by the fact that the matrix $\hat{\rho}_4$ to be decomposed is Hermitian. For this class of matrices (and for all normal matrices), the so-called geometric

multiplicity of each eigenvalue is guaranteed to be equal to its so-called algebraic multiplicity, i.e. these matrices are nondefective (see details in [48] p. 57, 58, 103). More explicitly, this means that each eigenvalue of $\hat{\rho}_4$ is here known to appear d_1 times at arbitrary locations on the diagonal of D_4 (algebraic multiplicity), since these eigenvalues are the same, in a different order, as in another eigendecomposition of the same matrix $\hat{\rho}_4$ (neglecting estimation errors), namely the eigendecomposition (1). Therefore, the dimension of the eigenspace associated with any eigenvalue of $\hat{\rho}_4$ is also equal to d_1 . So, when performing the eigendecomposition of $\hat{\rho}_4$, the considered decomposition algorithm should provide d_1 linearly independent eigenvectors for each eigenvalue, and we hereafter assume that practical eigendecomposition algorithms succeed in finding them (that was indeed the case in all the tests reported further in this paper). As an overall result, when performing the eigendecomposition of $\hat{\rho}_4$, 1) we get a diagonal matrix D_4 with $d = d_1 d_2$ eigenvalues that may be in an arbitrary order, and with each encountered value repeated d_1 times and 2) we get a unitary matrix V_4 whose columns are eigenvectors that have the above-defined properties.

As in Section II-A, we then apply a joint permutation to the diagonal elements of D_4 and to the columns of V_4 , so that the values corresponding to the diagonal elements of D_4 become in nonincreasing order. Considering the resulting complete set of values from the top to the bottom of the diagonal of the reordered version of D_4 , we thus get d_2 successive subsets, with the same value repeated d_1 times in each subset (in practice, these d_1 values may be slightly different, due to estimation errors), and with different and decreasing values from one subset to the next one. In other words, up to estimation errors, the reordered version of D_4 is nothing but the matrix ρ_1 of (17). Each subset of identical values along the diagonal of the obtained matrix (values equal to eigenvalue r_{m_1}) has an index m_1 , with $m_1 \in \{1, \dots, d_2\}$, and consists of elements with indices³

$$(m_1 - 1)d_1 + n_1, \quad \text{with} \quad n_1 \in \{1, \dots, d_1\}. \quad (20)$$

Moreover, the corresponding matrix, derived from V_4 , with reordered eigenvectors in its columns is here again denoted as \hat{U}_2 . Its subset of columns that also have the indices defined by (20) is a set of d_1 eigenvectors that form a basis of the d_1 -dimensional eigenspace of $\hat{\rho}_4$ associated with its eigenvalue r_{m_1} . This eigenspace, obtained in the first part of this method, is hereafter denoted as \mathcal{S}_{1,m_1} .

Importantly, \mathcal{S}_{1,m_1} also has the following relationship with the actual matrix U to be identified. Eigenvectors corresponding to distinct eigenvalues are orthogonal for a normal matrix (see Theorem 3) and hence especially for a Hermitian matrix (see also [48] p. 171). This has the following consequence, considering that (1) and (17) define an eigendecomposition of ρ_2 : each eigenvalue r_{m_1} of ρ_2 , with a multiplicity d_1 ,

³In this whole paper except Appendix K, the index of the first row and column of a matrix is equal to 1.

corresponds to a d_1 -dimensional eigenspace 1) that is orthogonal to the eigenspaces defined by all other eigenvalues and 2) that is the subspace defined by the columns of U that have the indices defined by (20). But this eigenspace is nothing but \mathcal{S}_{1,m_1} , since ρ_2 is equal to $\widehat{\rho}_4$ (up to estimation errors). This shows that this first part of our second type of methods does not yet succeed in separately identifying each column of U , but it succeeds in finding a basis for each of the d_2 subspaces \mathcal{S}_{1,m_1} that corresponds to a value m_1 , with $m_1 \in \{1, \dots, d_2\}$, and that is associated with the d_1 columns of U that have the indices defined by (20). We hereafter show how to extend that method so as to identify each column of U separately.

C. SECOND PART OF THE METHODS

The two important properties that we showed in Section III-B for the considered (possibly high) dimension $d = d_1 d_2$ are as follows. First, we proved that we can “partition” the set of d columns of U in d_2 subsets, in the sense that, in Section III-B, we identified each d_1 -dimensional subspace \mathcal{S}_{1,m_1} spanned by the columns of U that compose the subset with index m_1 . Second, we proved that we can select which partition we perform: the columns of U that are gathered in the same subset are those that correspond to the same eigenvalue of ρ_2 and hence $\widehat{\rho}_4$.

In the present section, we take advantage of these results to create another partition of the columns of U , in order to then jointly exploit these two partitions as explained further in Section III-D. We thus create a two-stage algorithm in the sense that it successively uses two eigendecompositions of density matrices estimated at the output of the process U , namely the eigendecompositions respectively described in Section III-B and in the present subsection. This should be contrasted with the algorithms of Section II, that are single-stage methods in the sense that they perform a single eigendecomposition.

More precisely, the input density matrix ρ_5 here applied to the considered unitary process is different from ρ_1 but, here again, it is diagonal, it contains d_2 different values that each appear d_1 times and these values are the same as in Section III-B. However, they are here placed in a different order: the set of values on the main diagonal of ρ_5 consists of a series of d_1 identical subsets, each of which successively contains the d_2 values r_1, \dots, r_{d_2} . The density matrix ρ_5 thus reads

$$\rho_5 = \begin{bmatrix} r_1 & 0 & \dots & & 0 & & & \\ & \ddots & & & & & & \\ & & r_{d_2} & & r_1 & & & \\ & & & & \ddots & & & \\ 0 & & & & & r_{d_2} & & \ddots \end{bmatrix}. \quad (21)$$

This may also be expressed as

$$\rho_5 = I_{d_1} \otimes \text{diag}(r) \quad (22)$$

with the same notations as in (18).

This input density matrix ρ_5 is used in the same way as in Section III-B. So, the density matrix ρ_6 of the corresponding process output may be derived from ρ_5 in the same way as in (1). An estimate $\widehat{\rho}_6$ of ρ_6 is derived by a QST algorithm and, if required by the considered QST algorithm, we preprocess $\widehat{\rho}_6$ in order to derive: 1) its Hermitian version $\widehat{\rho}_7$ (in the same way as in (38)) and then 2) its Hermitian and unit-trace version $\widehat{\rho}_8$ (in the same way as in (39)). We then perform an eigendecomposition of $\widehat{\rho}_8$. This yields a diagonal matrix D_8 containing its eigenvalues and a matrix V_8 whose columns are its associated eigenvectors.

We then apply a joint permutation to the diagonal elements of D_8 and to the columns of V_8 , so that the values corresponding to the diagonal elements of D_8 become in nonincreasing order. Here again, each of the d_2 successive subsets of d_1 identical values along the diagonal of the reordered version of D_8 (values equal to eigenvalue r_{m_2}) has an index m_2 , with $m_2 \in \{1, \dots, d_2\}$, and consists of elements with indices

$$(m_2 - 1)d_1 + n_2, \quad \text{with } n_2 \in \{1, \dots, d_1\}. \quad (23)$$

Moreover, the corresponding matrix, derived from V_8 , with reordered eigenvectors in its columns is denoted as \widehat{U}_3 ⁴. Its subset of columns that also have the indices defined by (23) is a set of d_1 eigenvectors that form a basis of the d_1 -dimensional eigenspace of $\widehat{\rho}_8$ associated with its eigenvalue r_{m_2} . This eigenspace, obtained in the second part of this method, is hereafter denoted as \mathcal{S}_{2,m_2} .

\mathcal{S}_{2,m_2} also has a relationship with the actual matrix U to be identified, but it is different from the relationship disclosed for \mathcal{S}_{1,m_1} in Section III-B. Here again, \mathcal{S}_{2,m_2} is the d_1 -dimensional subspace spanned by the d_1 columns of U that correspond to the eigenvalue r_{m_2} . However, here the indices of these columns are different from those of Section III-B: they are equal to the column indices of all occurrences of r_{m_2} in (21), that is

$$m_2 + n_2 d_1 \quad \text{with } n_2 \in \{0, \dots, d_1 - 1\}. \quad (24)$$

This shows that this second part of our second type of methods succeeds in finding a basis for each of the d_2 subspaces \mathcal{S}_{2,m_2} that: 1) corresponds to a value m_2 , with $m_2 \in \{1, \dots, d_2\}$, and 2) is associated with the d_1 columns of U that have the indices defined by (24). We hereafter show how to combine the properties of these subspaces \mathcal{S}_{2,m_2} and of the subspaces \mathcal{S}_{1,m_1} derived in the first part of this algorithm.

⁴In this whole paper, all the quantities of importance related to estimates of the considered process are denoted with the same letter and increasing indices 1, 2 and so on. When describing our first type of methods in Section II, for the sake of clarity we used detailed notations for these estimates, therefore with a first notation (with index 1) for the quantity before column reordering and a second notation (with index 2) for the quantity after column reordering. However, we then did not use the first notation. We here want to make it clear that, for the second type of methods described in the present section, we also consider two such quantities, namely before and after reordering. However, we do not introduce a notation for the quantity before reordering because, here again, we would not use it afterwards. Therefore, we here only introduce a single quantity, with an index equal to 3.

D. THIRD PART OF THE METHODS

We now consider all subspace intersections $\mathcal{S}_{1,m_1} \cap \mathcal{S}_{2,m_2}$, for $m_1 \in \{1, \dots, d_2\}$ and $m_2 \in \{1, \dots, d_2\}$. The subspaces \mathcal{S}_{1,m_1} and \mathcal{S}_{2,m_2} are each defined by a set of column vectors of U and we want each such pair of subspaces to share *only one* column vector (or possibly no columns for some of these intersections). When this condition is met, $\mathcal{S}_{1,m_1} \cap \mathcal{S}_{2,m_2}$ is equal to the one-dimensional subspace defined by this shared column vector, because U is unitary and all its column vectors are therefore orthogonal (see [48] p. 67). Moreover, we want the set of d_2^2 intersection column vectors thus created to yield all d columns of U (up to scale factors). This requires $d_2^2 \geq d$ and hence, due to (16):

$$d_1 \leq d_2. \quad (25)$$

Besides, the number d_2 of different eigenvalues of the input density matrix (as defined in Section III-B) is upper bounded by the value n_{max} , as explained above. Therefore, due to (25) and (16), the state space dimension d that can be handled by the methods proposed in the present section is upper bounded by:

$$d \leq (n_{max})^2. \quad (26)$$

This maximum space dimension is therefore much higher than the bound (15) faced with the methods of Section II, under the assumption that n_{max} here remains the same as with single-stage methods, as discussed above. In that case, the methods of the present section are much more attractive for handling high-dimensional spaces (but more complex).

In the remainder of this section, we only consider the case when

$$d_1 = d_2 \quad (27)$$

which makes the analysis simpler. Combining this condition with (16) yields

$$d = d_1^2 = d_2^2. \quad (28)$$

When d_2 is moreover set to its maximum value n_{max} , we obtain $d = (n_{max})^2$, so that we reach the upper bound defined by (26).

One then analyzes how the indices of the columns of U corresponding to \mathcal{S}_{1,m_1} (defined by (20)) are interleaved with the indices of the columns of U corresponding to \mathcal{S}_{2,m_2} (defined by (24)), for any given couple of values (m_1, m_2) , with $m_1 \in \{1, \dots, d_2\}$ and $m_2 \in \{1, \dots, d_2\}$. This shows that, whatever (m_1, m_2) , the sets of columns of U respectively associated with \mathcal{S}_{1,m_1} and \mathcal{S}_{2,m_2} share one and only one column, and that its index is

$$(m_1 - 1)d_1 + m_2. \quad (29)$$

Moreover, when m_1 and m_2 are varied over all their ranges $m_1 \in \{1, \dots, d_2\}$ and $m_2 \in \{1, \dots, d_2\}$, the resulting set of d_2^2 indices (29) spans all $d = d_1 d_2 = d_2^2$ columns of U . This approach therefore succeeds in identifying all columns of U , up to scale factors at this stage.

The practical algorithm proposed for implementing the above approach operates as follows. Successively for each

couple (m_1, m_2) , with $m_1 \in \{1, \dots, d_2\}$ and $m_2 \in \{1, \dots, d_2\}$, we need to determine a vector situated in the 1-dimensional intersection of the subspaces \mathcal{S}_{1,m_1} and \mathcal{S}_{2,m_2} . The data available in practice for defining \mathcal{S}_{1,m_1} consist of the set of columns of \widehat{U}_2 that have the indices defined by (20) and the data that define \mathcal{S}_{2,m_2} consist of the set of columns of \widehat{U}_3 that have the indices defined by (23). To determine this 1-dimensional subspace intersection, we here use the first direction provided by the standard Canonical Correlation Analysis, or CCA, e.g. described in [54] and directly available in the Matlab scientific software [55]. This approach is by the way closely related to the eigendecomposition tool, that is the core of the methods proposed in the present paper⁵.

By calculating the intersection $\mathcal{S}_{1,m_1} \cap \mathcal{S}_{2,m_2}$, we obtain one column vector of U , possibly up to an arbitrary complex factor, unless this vector is guaranteed to be normalized by the considered CCA tool. If it is not, we then reduce this factor to a phase factor, by dividing this intersection vector by its norm, so as to enforce its norm to become equal to one (again because U is known to be unitary and thus to have unit-norm column vectors).

All these normalized results of CCA are used to create an additional matrix related to the estimation of U and therefore denoted as \widehat{U}_4 : each application of CCA to a given couple (m_1, m_2) yields a normalized vector that is stored in the column of \widehat{U}_4 whose index is defined by (29). The matrix \widehat{U}_4 obtained at this stage is therefore equal to U up to an arbitrary phase factor in each of its columns (and up to estimation errors).

E. FOURTH PART OF THE METHODS

The properties of \widehat{U}_4 defined at the end of the previous section are exactly the same as those obtained in our single-stage methods for \widehat{U}_2 : see Section II-A, including (4). Therefore, the final stage of the method considered here consists of processing \widehat{U}_4 in the same way as we processed \widehat{U}_2 in Section II-B. This yields a matrix \widehat{U}_5 that here again succeeds in restoring U , up to only a global phase factor.

A pseudo-code of the version of our algorithm described in this Section III is provided in Algorithm 2. This algorithm is called EQPT2. Two variants (called EQPT3 and EQPT4) of two-stage QPT methods are moreover presented in Appendix J.

IV. PROPOSED MULTI-STAGE QPT METHODS

The QPT methods proposed in the previous sections can be extended as follows, by selecting density matrices ρ_1 of input mixed states that are diagonal, that contain *several*

⁵It should also be noted that an alternative to CCA, based on Singular Value Decomposition, and that allows one to determine subspace intersections, is available in [56]. It is a building block of the method called SIBIS, for “Subspace-Intersection Blind Identification and Separation”. Beyond its subspace-intersection tool, SIBIS has the following relationships with the present paper in terms of final goal. SIBIS performs 1) Blind Mixture Identification, or BMI [57]–[60], which is a type of classical system identification problem and is thus related to (the classical counterpart of) QPT and 2) Blind Source Separation, which is a problem closely connected to classical BMI.

occurrences of each value that appears on their diagonal and that have additional properties. More precisely, here again, each value that appears on the main diagonal of ρ_1 appears d_1 times, with $d_1 > 1$, and that diagonal contains d_2 different values, here possibly with $d_2 \neq d_1$. The number of rows of ρ_1 , equal to the dimension of the considered state space, is thus here again defined by (16). The new feature introduced here consists of storing all d_1 occurrences of any given diagonal value of ρ_1 in b_n blocks of adjacent rows, with each block consisting of b_s rows, and hence with

$$b_n b_s = d_1. \quad (30)$$

Besides, we consider the case when b_n , b_s and d_1 are powers of 2. We denote as b_ℓ the integer-valued logarithm of b_n in base 2: we have

$$b_n = 2^{b_\ell}. \quad (31)$$

We hereafter consider all possible integer values of b_ℓ , for a fixed value d_1 and varying values of b_n and b_s . In other words, we consider all linked powers of 2 for b_n and b_s , in their acceptable range. The minimum of b_ℓ is 0, corresponding to the minimum of b_n , equal to 1, and to the maximum of b_s , equal to d_1 . Similarly, the maximum of b_ℓ is equal to $\log_2 d_1$, corresponding to the maximum of b_n , that is equal to d_1 , while b_s reaches its minimum, equal to 1.

Moreover, these blocks are organized as follows: from the top to the bottom of the diagonal of ρ_1 , we have a block of values equal to r_1 , then a block of values r_2 , and so on until a block of values r_{d_2} , and then the same structure again and again, that is, blocks of values r_1, r_2, \dots, r_{d_2} (when there exist several blocks containing the same value, i.e. when $b_n > 1$). Here again, we request these possible values to be defined in decreasing order, i.e. $r_1 > r_2 > \dots > r_{d_2}$, and to take the same values as in (19). The two extreme cases of this general framework are nothing but the two specific cases that we already used for the above-defined two-stage methods: when setting $b_\ell = 0$ and hence $b_n = 1$ and $b_s = d_1$, we obtain the density matrix of (17) whereas with $b_\ell = \log_2 d_1$ and hence $b_n = d_1$ and $b_s = 1$, we get the density matrix of (21).

The main idea of the above-defined two-stage methods was to exploit intersections of two subspaces of eigendecompositions resulting from the above density matrices (17) and (21). Here, we extend this idea to general multi-stage methods, with $(\log_2 d_1 + 1)$ stages. To this end, we consider all $(\log_2 d_1 + 1)$ input density matrices that belong to the above-defined general framework, by considering all $(\log_2 d_1 + 1)$ possible values of b_ℓ , i.e. all integers from 0 to $\log_2 d_1$. Using the same approach as in Section III (that is, performing the eigendecomposition and reordering for the estimated output density matrix), for each value of b_ℓ and hence of b_n and b_s , we obtain a set of d_2 subspaces denoted as $\mathcal{S}_{b_\ell, m_{b_\ell}}$, with $m_{b_\ell} \in \{1, \dots, d_2\}$ (each index m_{b_ℓ} is used to define each subspace in the eigendecomposition of the stage b_ℓ of the algorithm proposed here; its correspondence with the structure of the input density matrix is not the same as

when we used the indices m_1 and m_2 in Section III). These subspaces $\mathcal{S}_{b_\ell, m_{b_\ell}}$ are defined in more detail in Appendix K. We then extend the approach of Section III by performing subspace intersections as follows. We successively consider all $d_2^{(\log_2 d_1 + 1)}$ possible values of the set of $(\log_2 d_1 + 1)$ subspace indices m_{b_ℓ} (with $m_{b_\ell} \in \{1, \dots, d_2\}$), i.e. we consider all possible values of the set of indices $\{m_0, \dots, m_{\log_2 d_1}\}$. For each such set of indices, we derive the intersection of the corresponding $(\log_2 d_1 + 1)$ subspaces $\mathcal{S}_{b_\ell, m_{b_\ell}}$. We thus form $d_2^{(\log_2 d_1 + 1)}$ subspace intersections. As in Section III-D, we want each of these intersections to be one-dimensional (or possibly to be restricted to the null vector for some of these intersections). In order to identify all d columns of U , the number of subspace intersections should be at least equal to d . Using (16), this condition reads

$$d_2^{\log_2 d_1} d_2 \geq d_1 d_2. \quad (32)$$

Taking the logarithm, in base 2, of that equation yields

$$\log_2 d_2 \geq 1 \quad (33)$$

that is

$$d_2 \geq 2. \quad (34)$$

In particular, for $d_2 = 2$, we have equalities in (34) back to (32) and the number $d_2^{(\log_2 d_1 + 1)}$ of intersections is exactly equal to the dimension (16). It should be noted that, unlike in the two-stage methods, we here do not face the constraints (25) and hence (26). This is because we pay the price by using a multi-stage, hence more complex, approach: the method proposed here potentially applies to any state space dimension d and any number d_2 of different eigenvalues (with (34)), provided we accept to set accordingly the value of d_1 , defined by (16), and hence the number $(\log_2 d_1 + 1)$ of stages of the method and of eigendecompositions to be performed (and, again, provided this method remains numerically accurate enough, despite its higher computational complexity).

Moreover, also in this multi-stage extension, we aim at reducing the number d_2 of different eigenvalues, because we thus hope to better succeed in assigning each estimated eigenvalue to the correct value among the possible ones, despite estimation errors. A very attractive feature of the approach proposed here is that it allows one to decrease d_2 to 2, thus leading to Dichotomic multi-stage Eigenanalysis-based QPT, or DEQPT, methods (where “dichotomic” refers to the fact that the complete set of eigenvalues is split into two subsets, with identical values in each subset).

In Appendix K-A we prove that, for $d_2 = 2$, the above-defined subspace intersections are each indeed restricted to one dimension and yield all columns of U (up to scale or phase factors). Moreover, we illustrate this property and thus the proposed complete multi-stage methods in Appendix K-B. Finally, Appendix K-C contains a pseudo-code for that multi-stage QPT method applicable to an arbitrary state space dimension and called EQPT5.

V. TEST RESULTS

To validate the EQPT1, EQPT2, EQPT3 and EQPT5 methods detailed in the previous sections, and to evaluate their accuracy, we performed numerical tests with data derived from a software simulation of the considered configuration. As mentioned in Section I, all the methods proposed in the present paper belong to the class of QPT methods that first perform a complete QST for each considered process output state and then exploit the results of these QST to achieve the core of QPT. The input of our QPT methods thus consists of estimates (more precisely, models of such estimates, as detailed below) of pure or mixed states provided by QST. Various QST methods were reported in the literature (see e.g. [1], [9], [11], [61]–[73]) and one may hereafter e.g. use any of the available QST methods compatible with the types of quantum states encountered in each of the QPT methods proposed in the present paper. Therefore, to here provide numerical results that define the accuracy of our QPT methods, we do not restrict this investigation to the use of a single QST method, from which the reader could not easily extrapolate to his preferred QST approach, with his preferred parameter values (especially, the number of times he prepares a copy of a considered input state and he performs a measurement for the corresponding output state), whereas these parameter values may have a strong influence on QPT performance. Instead, we create a numerical model of quantum state estimates with a given accuracy and we focus on the resulting accuracy of our QPT methods, not only to estimate these absolute accuracies, but mainly to determine which of these methods yields the best performance when they use the *same* accuracy for QST. This moreover allows us to investigate the numerical performance of our QPT methods over a wide range of conditions, by varying the accuracy of the modeled quantum state estimates.

It should also be noted that some papers from the literature focus on reducing the complexity of QST algorithms (see e.g. [72], [73]). The overall complexity of a QST-based QPT algorithm therefore does not necessarily come from its QST part, as opposed to its subsequent part that consists of using QST results for the core of QPT. This also motivates us to perform tests as explained above, in order to uncouple the investigation of the complexity of the core of QPT (e.g. expressed in terms of required CPU time) from that of QST.

More precisely, to model a ket estimate (e.g. for the ket $|\Psi_2\rangle$ of Section II-B), we compute its theoretical value in the considered conditions (e.g. using (6) with the input ket defined before (12) and a known process matrix U) and we add random, independent, complex-valued fluctuations to all components of this ket. Their real and imaginary parts are separately created with a random generator that has a probability density function that is uniform over the range $[-w/2, w/2]$, where the parameter w defines the magnitude of the modeled estimation fluctuations (their variance is thus equal to $w^2/12$). This parameter is hereafter varied so as to investigate the sensitivity of the proposed QPT methods to the magnitude of QST estimation errors. This simple

error model has the advantage of being easily interpretable. The error model for density matrix estimation is defined accordingly and is presented in Appendix L.

Each elementary test uses a randomly drawn $d \times d$ process matrix U , obtained as follows. We first create a $d \times d$ real-valued matrix with each element randomly, uniformly, drawn in the interval $[0, 1]$. We then perform a QR decomposition of this matrix (e.g. using one of the algorithms defined in [48] p. 112, [74] p. 223, [75]). This especially yields the so-called “Q factor” of that QR decomposition (see e.g. the software package [75]). This factor is guaranteed to be a unitary matrix (see [48] p. 112, [74] p. 223, [75]) and we therefore use it as our matrix U .

Each above-defined matrix U is used by feeding it with the process input states defined in the previous sections, computing the corresponding exact output states (e.g. using (1) and (6)), deriving their above-defined modeled estimates associated with QST and applying the considered QPT method to those estimates, so as to derive the process matrix estimate \widehat{U}_5 .

The criterion used to evaluate the performance obtained in such a test aims at measuring how close we get to the case when \widehat{U}_5 is equal to U up to a phase factor. The criterion used to this end is defined by first introducing

$$NMSE(U, \widehat{U}_5) = \min_{\theta} \left[\frac{1}{2d} \|U - e^{i\theta} \widehat{U}_5\|_F^2 \right] \quad (35)$$

where $\|\cdot\|_F$ stands for the Frobenius norm and where the phase θ is chosen so as to minimize this NMSE. The NMSE value resulting from this minimization may be shown to be equal to

$$NMSE(U, \widehat{U}_5) = \frac{1}{2d} \left[\|U\|_F^2 + \|\widehat{U}_5\|_F^2 - 2 |\text{Tr}(U^\dagger \widehat{U}_5)| \right]. \quad (36)$$

This criterion is a Normalized Mean squared Error (NMSE) since it is based on the sum of the squared moduli of the elements of the error matrix $(U - e^{i\theta} \widehat{U}_5)$, then normalized by a scale factor chosen so that the maximum value of this parameter is equal to one when U and \widehat{U}_5 are unitary (because their squared norms are then equal to d). The criterion that we eventually consider is the Normalized Root Mean Square Error (NRMSE) associated with the above NMSE:

$$NRMSE(U, \widehat{U}_5) = \sqrt{NMSE(U, \widehat{U}_5)}. \quad (37)$$

For each dimension d of the state space, the results reported below were obtained by running 100 above-defined elementary tests, each with a different, randomly drawn, process matrix U (except that we only performed 10 tests when applying the EQPT5 method to 11 qubits, as explained below). The performance figure then provided is the mean of $NRMSE(U, \widehat{U}_5)$ over all these tests. This protocol is repeated for various values of d .

The reported tests were carried out with a standard PC (Intel(R) Core(TM) i5-7500 CPU running at 3.40 GHz with 16 GB of RAM), using the Matlab software environment. As

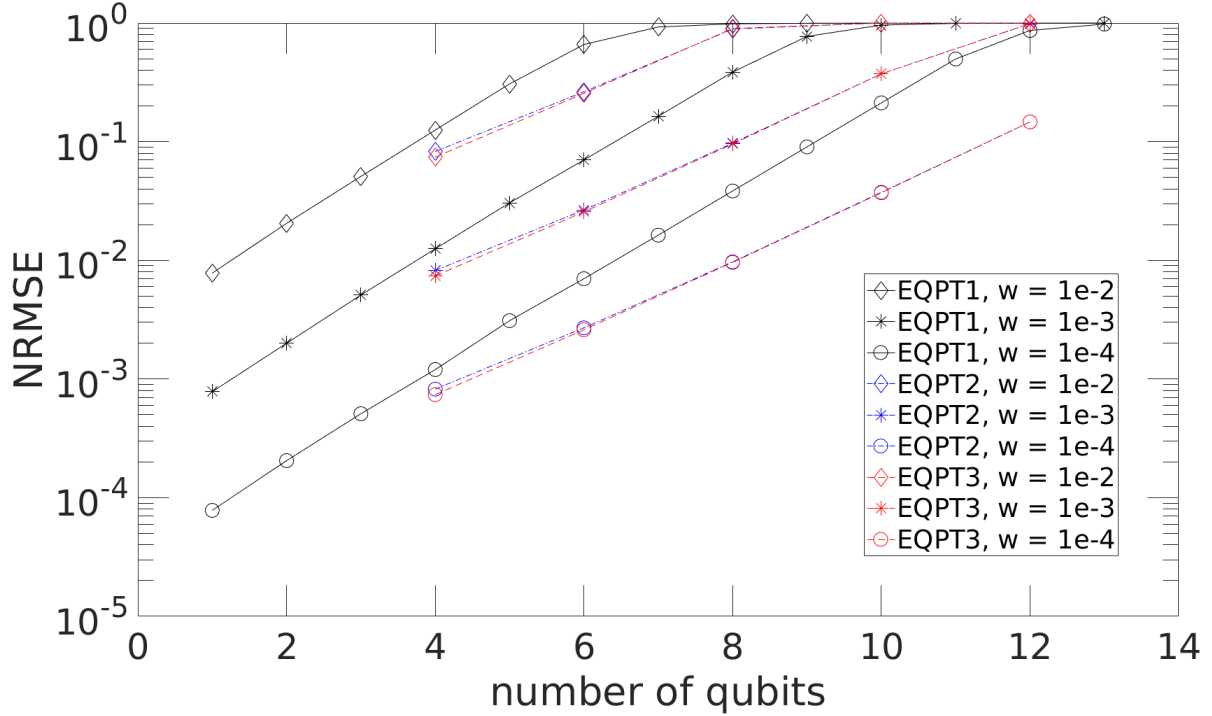


FIGURE 1. Normalized Root Mean Square Error (NRMSE) of estimation of process matrix U of proposed Quantum Process Tomography (QPT) methods EQPT1 (black solid lines), EQPT2 (blue dash-dotted lines) and EQPT3 (red dashed lines), vs. number q of qubits, for several values of the parameter w that defines the magnitude of the estimation errors of Quantum State Tomography (QST).

a first step, Fig. 1 shows the results thus obtained with our single-stage and two-stage methods, namely EQPT1 (black solid lines), EQPT2 (blue dash-dotted lines) and EQPT3 (red dashed lines). The results for EQPT1 are provided for all values of the state space dimension d that take the form $d = 2^q$, where q is the equivalent number of qubits, that is here varied from 2 to 13. $q = 13$ is the maximum number that was accepted in the considered hardware and software environment without running out of memory (for non-optimized code). The same approach applies to EQPT2 and EQPT3 except that, due to (28), only even values of q were considered. Moreover, for EQPT2 and EQPT3, performance turned out to often be somewhat degraded for the lowest possible state space dimension, namely $d = 4$, that corresponds to $q = 2$ qubits. This is not an issue, since EQPT2 and EQPT3 were developed to address higher values of d (EQPT1 can be used instead for lower values of d). Therefore, for better readability, the results of EQPT2 and EQPT3 for $q = 2$ are skipped in Fig. 1. It should also be noted that the complexity of the configurations that could be tested was limited by memory requirements, as stated above, hence not by the computational load of the proposed algorithms, that remained reasonable up to $q = 13$. For instance, for each of the 100 process matrix estimations, the average execution time used for a) creating data (thus only “modeling” QST instead of running a QST algorithm: see above), b) running the QPT algorithm and c) displaying

results, was as follows, respectively for EQPT1, EQPT2 and EQPT3: 1) $\simeq 1$ ms, 2.6 ms and 2.8 ms for $q = 4$ qubits, 2) 22 ms, 170 ms and 200 ms for $q = 8$ qubits and 3) 23 s, 180 s and 230 s for $q = 12$ qubits. The execution times for the other numbers of qubits are provided in Table 1.

The following conclusions can be drawn from Fig. 1, when comparing the proposed methods for any given QST quality, defined by the considered value of w . The two-stage methods EQPT2 and EQPT3 yield almost the same performance, with a slight advantage for EQPT3 (as expected from Appendix J), that is more significant for lower values of the space dimension d . Moreover, these two-stage methods always yield better and often much better performance than the single-stage method EQPT1, as expected from the beginning of Section III. Up to a certain space dimension d , the gap between these two types of methods increases with the space dimension and hence with the associated number q of qubits: whereas all methods yield linear variations of the logarithm of NRMSE with respect to q (i.e. logarithm of d), the slope of these variations is significantly lower for EQPT2 and EQPT3, and these methods already start with a lower NRMSE than EQPT1 for the lowest values of d . Depending on the considered conditions, the EQPT2 and EQPT3 methods decrease the NRMSE by a factor up to 6, and hence the NMSE by a factor up to 36, as compared with EQPT1. Moreover, for the lowest QST error magnitude considered in these tests, for all analyzed state space dimensions, EQPT2 and EQPT3

yield an NRMSE limited to about 10^{-1} and hence an NMSE limited to about 10^{-2} .

We now move to the multi-stage method EQPT5, whose performance is shown in Fig. 2 (red dashed lines), together with the results already provided above for EQPT1 (black solid lines) and EQPT2 (blue dash doted lines). The results for EQPT5 are reported for values of the state space dimension d that take the form $d = 2^q$, where q is the equivalent number of qubits, varied as follows. For a large q , EQPT5 yields a significantly higher computational complexity than the single-stage and two-stage methods, due to the higher number of eigendecompositions it performs and to the associated program structure (recursive function with a binary tree structure, as explained in Appendix K). Unlike for the previous proposed methods, the applicability of EQPT5 to a large number of qubits was therefore more limited by its computational load than by its memory requirements, when using the considered basic hardware and software means. Therefore, to keep a reasonable simulation duration (for *all* estimations of the process matrix), EQPT5 was only tested up to $q = 10$ qubits when performing 100 above-defined elementary tests, and also for $q = 11$ qubits but then with only 10 elementary tests. Moreover, as with EQPT2, we hereafter skip the results for a low dimension, that is for $d \leq 4$, which is not the case of interest for a multi-stage method. In the considered range of space dimensions, the above-defined average execution time per process matrix estimation was e.g. as follows for EQPT5: 5.4 ms for $q = 4$ qubits, 4.4 s for $q = 8$ qubits, 490 s \simeq 8 mn for $q = 10$ qubits and 7600 s \simeq 2 h 07 mn for $q = 11$ qubits. The execution times for the other numbers of qubits are provided in Table 1.

Fig. 2 yields the following conclusions for EQPT5. For the lowest considered values of the space dimension, EQPT5 starts with a somewhat higher NRMSE than EQPT1 and EQPT2. But, an attractive feature of EQPT5 is that its NRMSE then increases more slowly than those of the other methods, with respect to the space dimension. This again yields *linear* variations of the logarithm of NRMSE with respect to the number of qubits. EQPT5 thus outperforms the other two methods for higher space dimensions, and the gap between them increases with that dimension, up to a certain dimension. EQPT5 is thus attractive for high space dimensions, so that it actually reaches the goal for which it was designed. Depending on the considered conditions, EQPT5 decreases the NRMSE by a factor up to 3.2, and hence the NMSE by a factor up to more than 10, as compared with EQPT2. Moreover, for the lowest QST error magnitude considered in these tests, for all analyzed state space dimensions (which are slightly lower than those considered above for EQPT1 and EQPT2, however), EQPT5 yield an NRMSE limited to around 3.2×10^{-2} and hence an NMSE limited to around 10^{-3} .

VI. CONCLUSION AND FUTURE WORKS

Quantum Process Tomography (QPT) is a research topic of major interest, due to its importance for experimentally

characterizing the actual behavior of quantum gates. In the present paper, we addressed QPT configurations that have two features: first, we consider unitary processes, and second, we aim at developing QPT methods that are applicable to a high state space dimension, corresponding to a significant number of qubits, as explained in Section I.

Since the considered process is unitary, its input-output relationship takes a specific form, that suggests that eigenanalysis may be used to estimate at least part of the parameters of the process matrix. We first built upon that idea, and we then extended it so as to also estimate the other process parameters that a plain eigenanalysis cannot estimate. This resulted in a first class of QPT methods (including EQPT1), that are stated to be single-stage since they only require one eigendecomposition.

The above approach may however be expected to yield limited performance when considering high-dimensional state spaces, due to the estimation errors of the Quantum State Tomography (QST) that it uses as a building block. We very significantly reduced this problem by introducing multi-stage eigenanalysis-based extensions of our approach, where the term “multi-stage” refers to the fact these methods successively perform several eigendecompositions. We explained in detail how two-stage methods (especially EQPT2 and EQPT3) operate, and then how to extend them to an arbitrary number of stages in order to minimize their sensitivity to QST errors (especially with the dichotomic EQPT5 method).

The relevance of this approach was validated by means of numerical tests performed with a simulated version of this QPT problem. This especially showed that, depending on the considered conditions, the tested two-stage methods (EQPT2 and EQPT3) decrease the NMSE by a factor up to 36, as compared with the tested single-stage method (EQPT1). Moreover, for the lowest QST error magnitude considered in these tests, for all analyzed state space dimensions, the two-stage methods yield an NMSE limited to about 10^{-2} . Besides, the multi-stage dichotomic EQPT5 method may yield a higher accuracy (NMSE decreased by a factor up to 10 as compared with the two-stage EQPT2 method and NMSE limited to about 10^{-3} in almost the same conditions as above) but at the expense of a higher computational load.

We here had to restrict ourselves to tests performed on a standard PC. Our future works will therefore especially include additional tests, performed on a much more powerful platform, to derive the performance of our methods for a significantly higher number of qubits. Anyway, the configurations reported in the present paper already involve a quite significant number of qubits (up to 11 to 13, depending on the considered method) and hence a high state space dimension d (up to a few thousands) as compared with various investigations from the literature, in particular with only $d = 5$ in [3] that also deals with unitary processes. Our tests also showed that the applicability of our single-stage and two-stage methods was not limited by their complexity in terms of computational cost, unlike various alternative QPT methods, but only by the memory size available on the

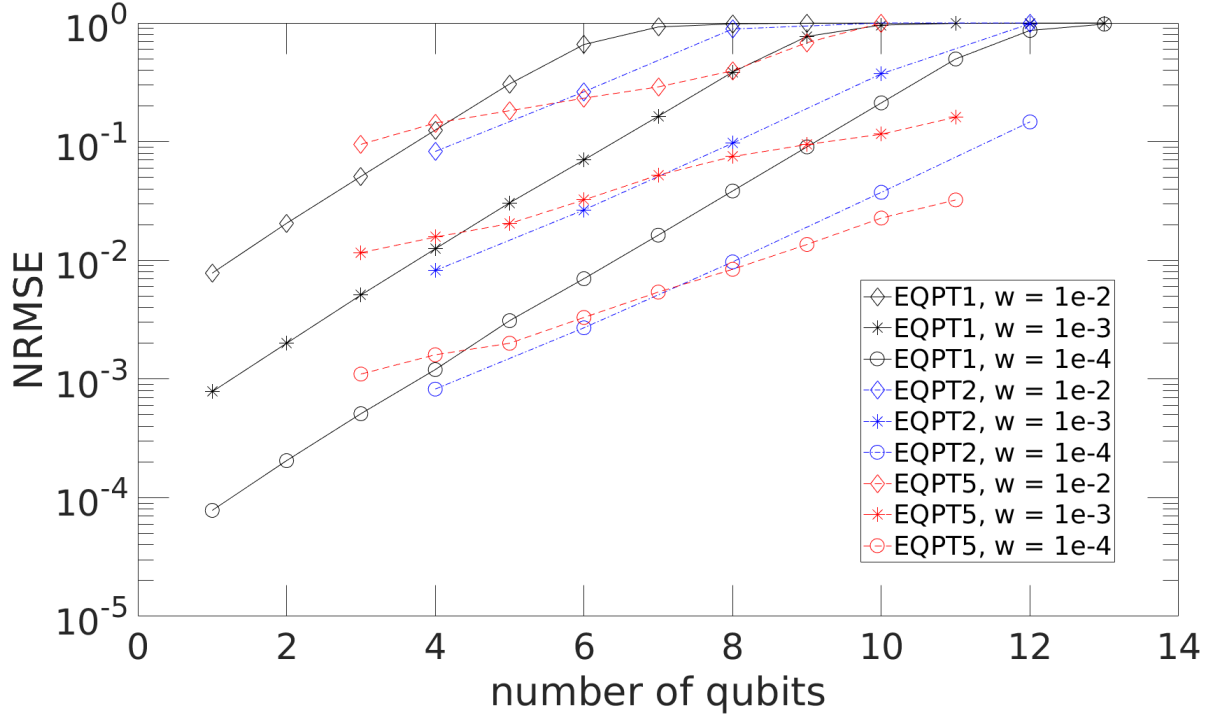


FIGURE 2. Normalized Root Mean Square Error (NRMSE) of estimation of process matrix U of proposed Quantum Process Tomography (QPT) methods EQPT1 (black solid lines), EQPT2 (blue dash dotted lines) and EQPT5 (red dashed lines), vs. (number q of qubits) for several values of the parameter w that defines the magnitude of the estimation errors of Quantum State Tomography (QST).

platform that was used for running them. Our dichotomic multi-stage methods have the opposite features.

APPENDIX A CONNECTIONS BETWEEN OUR QPT METHODS AND CLASSICAL SIGNAL PROCESSING

As stated in Section I, the type of QPT approaches proposed in this paper has connections with works that were previously reported in the classical domain. These connections may be defined as follows. QPT may be considered as the quantum version of so-called (classical) system identification [1]. The latter classical problem consists of estimating the parameter values of a transform from the input to the output of a system. That system may have multiple inputs, so that it then performs a combination of them. In the classical framework, such a combination is called a mixture. The classical problem then considered in the literature is therefore also referred to as mixture identification and it especially includes blind mixture identification, or BMI [57]–[60]. This terminology should be used with care when also considering the quantum domain, because the above classical “mixtures” have nothing to do with the “statistical mixtures”, i.e. “mixed states”, faced in the quantum domain and used further in this paper. Only considering previous works in the *classical* domain at this stage of our discussion, the above-mentioned BMI has a close relationship with source separation, especially including blind source separation, or BSS [50], [53], [57], [58],

[76]–[78]. BSS does not focus on identifying the transform performed by the above, i.e. direct, system itself, but mainly on deriving an estimate of the inverse of that transform, so as to apply it to the outputs of the above direct system and to thus restore the unknown source signals that form the input of the direct system. This relationship between BMI and BSS even appears in the name of the well-known SOBI method [79], which stands for “Second-Order Blind Identification”, whereas it is claimed to be a BSS method. The term “Second-Order” here refers to the fact that this method applies to random signals and uses the statistical properties of the measured signals, more precisely their usual second-order statistical parameters that consist of their covariance matrices involving different time delays between signals.

So far, we especially discussed how SOBI-like methods and the methods proposed in the present paper are connected in terms of the nature of data processing problems that they address. These two types of methods also have relationships in terms of the approaches that they use to solve the considered problems. More precisely, in classical BSS/BMI, when the transform performed by the direct system is linear (and memoryless) and its identification is performed by using the above-mentioned second-order statistics of the output signals of the direct system, an equation similar to (1) is obtained [60], [79]–[82]. That classical counterpart of the structure of (1) was already exploited to perform classical BSS/BMI by means of several methods based on eigendecomposition.

The real-valued version of the basic structure of (1) was first used in [60], [80] together with a required modified form of this equation (a related approach also appears in [82]). It was then extended in [79], by combining it with more than one modified form of this equation, to obtain a more robust method. Another version [81] aims at extending that type of approach from the standard case of stationary time-domain source signals to nonstationary time-domain sources. That version eventually uses complex-valued signals (whereas the mixing transform remains real-valued) because one moves to the Fourier domain.

APPENDIX B CREATING A MIXED STATE THAT HAS A DIAGONAL DENSITY MATRIX

The algorithm proposed in Section II-A uses an input density matrix ρ_1 that is diagonal. It should be noted that, when one considers that one is able to create a pure state, then, creating the type of state considered here is not a problem, as will now be shown. We here consider the approach initially used by von Neumann in [83] to define a statistical mixture: such a state is expressed as being composed of a set of pure states, each of them being associated with a probability of occurrence. Then, to create experimental data corresponding to the state defined by the diagonal density matrix ρ_1 , one just has to repeatedly, randomly, select one of the pure states that form the considered basis of the state space, moreover selecting the k th basis state with a probability that is equal to the k th value on the diagonal of ρ_1 . This simplicity of implementation is worth noting because, in contrast, the authors of [3], [44] consider that using a mixed input state is too complex (maybe because they have non-diagonal density matrices in mind), so that they choose to restrict themselves to pure states, which has the drawback of requesting many such multiqubit input states, as opposed to only two multiqubit input states in the complete approach that we here start to describe (namely the mixed state with a density matrix ρ_1 considered here, and then the pure state $|\Psi_1\rangle$ in Section II-B). Beyond their relationship based on considering (1), our approach and the one in [44] are therefore quite different.

APPENDIX C PREPROCESSING STEPS OF THE SINGLE-STAGE QPT ALGORITHM

The first part of our single-stage algorithm, described in Section II-A, is based on an estimated density matrix $\hat{\rho}_2$ provided by a QST algorithm. If this estimate $\hat{\rho}_2$ is not guaranteed to be Hermitian due to the estimation errors of the considered “external” (i.e. external to *our* QPT) QST algorithm, a first recommended preprocessing step of our method consists of deriving a Hermitian estimate $\hat{\rho}_3$ from $\hat{\rho}_2$. This may be achieved by computing the Hermitian part of $\hat{\rho}_2$, that is (see [48] p. 109 or [50] p. 343 for its real-valued counterpart):

$$\hat{\rho}_3 = \frac{1}{2} \left(\hat{\rho}_2 + \hat{\rho}_2^\dagger \right). \quad (38)$$

Similarly, the actual matrix ρ_2 is known to have a trace equal to 1, since it is a density matrix (see e.g. [1] p. 101, [84] p.

73, [45] p. 283). Therefore, if its estimate ($\hat{\rho}_2$ or) $\hat{\rho}_3$ obtained so far is not guaranteed to have a unit trace due to QST estimation errors, a second recommended preprocessing step of our method consists of deriving a (still Hermitian and moreover) unit-trace estimate $\hat{\rho}_4$ from ($\hat{\rho}_2$ or) $\hat{\rho}_3$, by dividing all its elements by its trace:

$$\hat{\rho}_4 = \frac{\hat{\rho}_3}{\text{Trace}(\hat{\rho}_3)}. \quad (39)$$

Similarly, the second part of our single-stage algorithm, described in Section II-B, uses an estimated ket $|\hat{\Psi}_2\rangle$, provided by a QST algorithm. If the considered QST algorithm does not guarantee that the norm of $|\hat{\Psi}_2\rangle$ is equal to 1, a recommended pre-processing step of our QPT method consists of dividing $|\hat{\Psi}_2\rangle$ by its norm.

APPENDIX D PREFERRED INPUT DENSITY MATRIX FOR THE FIRST PART OF THE SINGLE-STAGE QPT ALGORITHM

In the first step of our first method defined in Section II-A, we preferably use the value of ρ_1 defined as follows. The values on its diagonal are the eigenvalues of the considered density operator ρ_2 , they are real and non-negative and their sum is equal to one (see e.g. [1] p. 101). As shown in Section II-A, the proposed method assumes that these eigenvalues are different and ordered, and it is based on reordering the eigenvalues in the eigendecomposition of the estimated output density matrix and on permuting the eigenvectors accordingly. Therefore, if using quite close actual eigenvalues when choosing ρ_1 , one may fear that the corresponding estimated eigenvalues obtained for the output density matrix be permuted due to estimation errors, so that the corresponding eigenvectors may then be permuted accordingly. This is a major problem, because the intermediate estimate \hat{U}_2 related to the considered process, obtained at the output of this first step of our QPT method, is primarily based on these eigenvectors. In this paper, we handle this problem as follows: first, for the method imposed in Section II-A, we select the value of ρ_1 in order to limit that problem to the greatest extent that is possible within the frame of that method; then, in Sections III and IV, we propose more advanced methods that allow one to further reduce that problem. So, for the method considered here, we choose eigenvalues that are uniformly distributed (i.e. multiples of the same step, with zero excluded), so as to maximize the gap between any two adjacent values. Moreover constraining them to be positive, with a sum equal to one and in decreasing order as explained above, it is easily shown that one obtains the following values for the diagonal elements $\rho_{1,kk}$ of ρ_1 :

$$\rho_{1,kk} = \frac{2(d-k+1)}{d(d+1)} \quad k \in \{1, \dots, d\}. \quad (40)$$

APPENDIX E PREFERRED INPUT KET FOR THE SECOND PART OF THE SINGLE-STAGE QPT ALGORITHM

In the second step of first method defined in Section II-B, we select the input ket $|\Psi_1\rangle$ as follows. Based on the condition on nonzero components provided in Section II-B for $|\Psi_1\rangle$, we preferably select a state $|\Psi_1\rangle$ with all component moduli as high as possible. Considering positive real-valued components and taking into account that $|\Psi_1\rangle$ has unit norm, this yields a single solution: all components of $|\Psi_1\rangle$ in the considered basis are equal to $1/\sqrt{d}$.

APPENDIX F MATHEMATICAL DEFINITIONS AND PROPERTIES

Definition 1: The element-wise division \oslash for vectors is defined as follows. Considering two vectors u and v , respectively with k th elements u_k and v_k , the quantity $u \oslash v$ is the vector whose k th element is equal to u_k/v_k .

Theorem 1: Every normal matrix $A \in M_n$ can be written as

$$A = U \Lambda U^\dagger, \quad (41)$$

where $U \in M_n$ is unitary and $\Lambda \in M_n$ is a diagonal matrix whose main diagonal entries are the eigenvalues of A (M_n is the set of n -by- n complex matrices).

Proof 1: See [48] p. 157 (e). See also [48] p. 101 for unitarily diagonalizable matrices (every normal matrix is unitarily diagonalizable) and the spectral theorem for normal matrices. In particular, this implies the spectral theorem for Hermitian matrices: see [48] p. 104. ■

Theorem 2: If $A \in M_n$ reads

$$A = P D P^{-1} \quad (42)$$

where $D \in M_n$ is a diagonal matrix and $P \in M_n$ is invertible then, for any index $k \in \{1, \dots, n\}$, the k th column of P is an eigenvector of A and the associated eigenvalue is the k th value on the diagonal of D .

Proof 2: Right-multiplying (42) by P yields

$$AP = PD. \quad (43)$$

For any index $k \in \{1, \dots, n\}$, the k th column of the matrix equation (43) reads

$$Av_k = \lambda_k v_k \quad (44)$$

where v_k is the k th column of P and λ_k is the k th element on the diagonal of D . Eq. (44) shows that v_k is an eigenvector of A and that the associated eigenvalue is λ_k . ■

Theorem 3: If $A \in M_n$ is normal, and if x and y are eigenvectors corresponding to distinct eigenvalues, x and y are orthogonal.

Proof 3: See [48] p. 103. ■

Theorem 4: A best least-squares approximation of a given matrix $A \in M_n$ by a unitary matrix $U_A \in M_n$ is given by $U_A = VW^\dagger$, where $A = V\Sigma W^\dagger$ is a singular value decomposition (SVD) of A .

Proof 4: See [48] p. 431. ■

APPENDIX G A VARIANT FOR THE FIRST PART OF SINGLE-STAGE QPT METHODS

We here again consider the first part of single-stage QPT methods. As in the variant that we proposed in Section II-A for that first part, we here use a mixed input state, represented by the density matrix ρ_1 . However, for the sake of generality, this matrix is here not any more constrained to be diagonal. It is still Hermitian and therefore unitarily diagonalizable. In the version considered here, as in Section II-A, we request all its eigenvalues to be different. That input density matrix ρ_1 is here requested to be known (i.e. fixed a priori or estimated from copies of that state, so that this variant is supervised or semi-supervised).

Using the same properties of eigendecomposition as in Section II-A, we consider all unitarily diagonalized forms of ρ_1 that have the following properties:

- 1) The eigenvalues are in a known order along the diagonal of ρ_1 . Without loss of generality, we hereafter consider the case when they are in decreasing order.
- 2) All eigenvectors have unit norm.

All these eigendecompositions of ρ_1 may be expressed as

$$\rho_1 = U_{I1} \rho_{I1D} U_{I1}^\dagger \quad (45)$$

where U_{I1} and ρ_{I1D} are respectively a unitary matrix and a diagonal matrix associated with that first input of the considered process.

Starting from a given ρ_1 , the first step of the algorithm proposed in the present section consists of determining one (arbitrary) of these decompositions (45) meeting the above-defined conditions. This is performed by 1) running an eigendecomposition algorithm, then 2) reordering the values in the matrix obtained for ρ_{I1D} if they are not directly provided in decreasing order by the considered eigendecomposition algorithm, 3) reordering the columns of the matrix obtained for U_{I1} accordingly and 4) dividing these columns by their norms if the considered practical eigendecomposition algorithm is not guaranteed to yield unit-norm vectors. Thus, we especially get a known value U_{I1} (which contains indeterminacies consisting of a phase factor separately for each of its columns). U_{I1} is used in the second part of this version of our algorithm: see Appendix I.

Besides, using (45), Equation (1) may be expressed as

$$\rho_2 = U_g \rho_{I1D} U_g^\dagger \quad (46)$$

where the global unitary matrix

$$U_g = U U_{I1} \quad (47)$$

includes the effect of the eigendecomposition of ρ_1 , in addition to the considered process U .

Formally, (46) addresses exactly the same problem as in Section II-A (see (1) with a diagonal ρ_1), but now with a diagonal input density matrix ρ_{I1D} and a process U_g (that is also unitary). We can therefore apply the algorithm and results of Section II-A to this reformulated problem, i.e.,

briefly, we diagonalize $\widehat{\rho}_4$ and we then reorder the eigenvalues (in the same order as in ρ_{I1D}) and associated normalized eigenvectors. This guarantees that the algorithm of Section II-A here provides an estimate \widehat{U}_2 that restores U_g up to a phase factor for each of its columns, with (5) here replaced by

$$\widehat{U}_2 = U_g D_\phi \quad (48)$$

$$= U U_{I1} D_\phi \quad (49)$$

where D_ϕ is again a diagonal matrix that contains unknown phase factors $e^{\phi_1}, \dots, e^{\phi_d}$ on its main diagonal.

As opposed to the basic version of the first step defined in Section II-A, the estimate \widehat{U}_2 here contains the effect of U_{I1} in addition. The second part of the method must then be modified accordingly, as compared with its basic version defined in Section II-B. A solution to this problem is provided in Appendix I.

APPENDIX H A VARIANT FOR THE SECOND PART OF SINGLE-STAGE QPT METHODS

In the framework of single-stage QPT methods that include a first part as defined in Section II-A, we here again consider the associated second part, that aims at estimating the phase factors $e^{i\phi_1}, \dots, e^{i\phi_d}$, by using a second input state of the considered process. The method that we proposed in Section II-B for that second part uses a pure input state defined by a ket $|\Psi_1\rangle$. However, a mixed input state having a density matrix ρ_5 may be used instead, as will now be shown. As $|\Psi_1\rangle$ in Section II-B, the input density matrix ρ_5 is here supposed to be initially known (supervised case) or estimated by using part of the available copies of that state (semi-supervised case).

The input state ρ_5 yields a state ρ_6 at the output of the considered process, and these two states have the same relationship as in (1). In practice, what is available, thanks to QST, is an estimate $\widehat{\rho}_8$ of ρ_6 , here again after it has been pre-processed, if required, so as to be Hermitian and to have unit trace. Thus, up to estimation errors, $\widehat{\rho}_8$ meets the condition

$$\widehat{\rho}_8 = U \rho_5 U^\dagger. \quad (50)$$

Then, knowing $\widehat{\rho}_8$ and \widehat{U}_2 obtained in the first part of our algorithm (see Section II-A), the next step of our algorithm here consists of combining them to form

$$\rho_9 = \widehat{U}_2^\dagger \widehat{\rho}_8 \widehat{U}_2. \quad (51)$$

This may be seen as the extension, to a mixed state, of the quantity (9) in the variant of the present method that uses a pure input state instead: for the latter type of state, $\widehat{\rho}_8$ reduces to

$$\widehat{\rho}_8 = |\widehat{\Psi}_2\rangle\langle\widehat{\Psi}_2| \quad (52)$$

and the state $|\Psi_3\rangle$ considered in Section II-A corresponds to $\rho_9 = |\Psi_3\rangle\langle\Psi_3|$. Combining the latter expression with (9) and using (52), the resulting expression of ρ_9 is fully compatible with its extension (51) to an arbitrary mixed input state considered here.

Combining (50), (51) and (5), with U unitary, yields

$$\rho_9 = D_\phi^* \rho_5 D_\phi. \quad (53)$$

This shows that a diagonal matrix ρ_5 cannot be used in this approach, because all three matrices in the right-hand term of (53) are then diagonal, so that D_ϕ^* and D_ϕ cancel out and (53) reduces to

$$\rho_9 = \rho_5 \quad (54)$$

and ρ_9 does not yield any information about the phase factors in D_ϕ . This is not surprising because all the information that can be extracted with a diagonal input density matrix was already extracted by using such a matrix in the first part of our algorithm (see Section II-A). We therefore consider a non-diagonal matrix ρ_5 hereafter.

Whatever the input density matrix ρ_5 , denoting ρ_{kl} its elements, (53) yields (again up to estimation errors)

$$\rho_9 = \begin{bmatrix} \rho_{11} & \rho_{12} e^{i(\phi_2 - \phi_1)} & \dots & \rho_{1d} e^{i(\phi_d - \phi_1)} \\ \dots & & & \dots \end{bmatrix}. \quad (55)$$

Therefore, we consider a value of ρ_5 that is arbitrary except that all the elements of its first row are nonzero (this method may be adapted to the case when another row only has nonzero elements). The next step of our algorithm consists of computing the quantity

$$[\rho_9]_{1\bullet} \otimes [\rho_5]_{1\bullet} \quad (56)$$

where $[\cdot]_{1\bullet}$ represents the row vector equal to the first row of the considered matrix (i.e. row 1 and all columns, or “columns \bullet ”). Thanks to (55), we have

$$[\rho_9]_{1\bullet} \otimes [\rho_5]_{1\bullet} = [1, e^{i(\phi_2 - \phi_1)}, \dots, e^{i(\phi_d - \phi_1)}] \quad (57)$$

and hence

$$\text{diag}(([\rho_9]_{1\bullet} \otimes [\rho_5]_{1\bullet})^*) = e^{i\phi_1} D_\phi^*. \quad (58)$$

The next step of our algorithm therefore consists of computing

$$\widehat{U}_5 = \widehat{U}_2 \text{diag}(([\rho_9]_{1\bullet} \otimes [\rho_5]_{1\bullet})^*) \quad (59)$$

$$= \widehat{U}_2 \text{diag}((\widehat{U}_2^\dagger \widehat{\rho}_8 \widehat{U}_2)_{1\bullet} \otimes [\rho_5]_{1\bullet})^* \quad (60)$$

where (60) results from (51) and defines the complete processing performed in this second part of our algorithm, starting from the estimate \widehat{U}_2 of U obtained in the first part of the algorithm and combining it with the density matrices ρ_5 and $\widehat{\rho}_8$ used in that second part.

Combining (59), (58) and (5) yields

$$\widehat{U}_5 = e^{i\phi_1} U \quad (61)$$

i.e. \widehat{U}_5 succeeds in restoring U (once again, up to a global phase factor that has no physical consequences and up to the estimation errors that were mentioned above but implicit in the above equations).

APPENDIX I ANOTHER VARIANT FOR THE SECOND PART OF SINGLE-STAGE QPT METHODS

In the framework of single-stage QPT methods, we here again consider the case when the first part is defined as in Appendix G. We present an associated solution for the second part of the method, using a pure input state defined by a ket $|\Psi_1\rangle$. $|\Psi_1\rangle$ is requested to be known, i.e. fixed a priori (supervised case) or estimated from a subset of its copies (semi-supervised case).

Starting with the same approach as in Section II-B, this here again yields the output ket estimate (8). Our algorithm then computes $|\Psi_3\rangle$ defined by (9), as in Section II-B, but now with \widehat{U}_2 that meets (49). Combining (49) with (9) and (8) and considering that U is unitary (hence $U^\dagger U = I$), we get

$$|\Psi_3\rangle = e^{i\theta} D_\phi^* |\Psi_4\rangle \quad (62)$$

where we introduce

$$|\Psi_4\rangle = U_{I1}^\dagger |\Psi_1\rangle \quad (63)$$

which is a known quantity. Comparing (62) with (10) shows that $|\Psi_4\rangle$ here replaces the ket $|\Psi_1\rangle$ used in the method of Section II-B (which is coherent with the fact that the latter method is a reduced form of the present one, for the case when ρ_1 is diagonal and hence U_{I1} is the identity matrix). The remainder of the present method is then derived by modifying the end of the method of Section II-B accordingly: here using

$$\widehat{U}_5 = \widehat{U}_2 \text{ diag}(|\Psi_3\rangle \otimes |\Psi_4\rangle) U_{I1}^\dagger \quad (64)$$

it may be shown in the same way as in Section II-B that we here again get (14), i.e. \widehat{U}_5 here again succeeds in restoring U , up to a global phase factor (and again up to estimation errors).

APPENDIX J VARIANTS OF TWO-STAGE QPT METHODS

Since the columns of \widehat{U}_4 are estimated independently, one may fear that they are not exactly orthogonal, due to estimation errors. Then, \widehat{U}_4 and hence \widehat{U}_5 are not unitary, although they should be because they aim at estimating U , that is constrained to be unitary. A first solution to this problem consists of postprocessing \widehat{U}_4 , so as to determine a best least-squares unitary approximation of \widehat{U}_4 . An algorithm that may be used to this end is defined by Theorem 4. The resulting modified QPT method is called EQPT3 hereafter. Its pseudo-code is provided in Algorithm 3. A slightly different version consists of finding a unitary approximation of \widehat{U}_5 instead of \widehat{U}_4 . The resulting QPT method is called EQPT4. Its pseudo-code is provided in Algorithm 4.

APPENDIX K ADDITIONAL INFORMATION FOR THE PROPOSED MULTI-STAGE METHODS

A. RELEVANCE OF THE METHODS

In this appendix, we first prove that the approach with $d_2 = 2$ that we proposed in Section IV, based on subspace intersections, is relevant.

Each subspace $\mathcal{S}_{b_\ell, m_{b_\ell}}$ defined in Section IV is associated with a set of columns of the process matrix U to be identified, in the following sense. We consider a given arbitrary stage of our algorithm, defined by the index b_ℓ , and the subset of columns of U that correspond to (i.e. that have the same column indices as) a given arbitrary diagonal value $r_{m_{b_\ell}}$ of the input density matrix ρ_1 when forming (1). This subset of columns of U and $r_{m_{b_\ell}}$ are defined by the index $m_{b_\ell} \in \{1, 2\}$. We then have the following property: the eigendecomposition plus reordering algorithm proposed in Section IV yields a set of column vectors associated with b_ℓ and m_{b_ℓ} , that form a basis of a subspace denoted as $\mathcal{S}_{b_\ell, m_{b_\ell}}$, and that subspace is also the subspace spanned by the columns of U associated with the index m_{b_ℓ} in the above-defined sense.

The analysis of the indices of these columns presented in the present appendix is made easier by introducing the following modified notations, related to the expression of these indices in base 2, which is motivated by the structure of the matrix ρ_1 based on powers of 2 that was introduced in Section IV:

- The index of the first row and first column of ρ_1 and U is here equal to 0 (instead of 1 in the other parts of this paper).
- Each variable m_{b_ℓ} , used to split in two subsets the columns of ρ_1 , takes the values 1 and 2 (because here $d_2 = 2$). With this, we here associate another binary variable, that takes the values 0 and 1, namely $\mu_{b_\ell} = m_{b_\ell} - 1$.
- When using the variable μ_{b_ℓ} , the subspaces are denoted with the letter \mathcal{T} , to avoid any misunderstanding with the notation $\mathcal{S}_{b_\ell, m_{b_\ell}}$ used above, especially when considering explicit numerical values of their indices: for instance, $\mathcal{T}_{0,0}$ is nothing but $\mathcal{S}_{0,1}$. More generally speaking, we have $\mathcal{T}_{b_\ell, \mu_{b_\ell}} = \mathcal{S}_{b_\ell, m_{b_\ell}}$, whatever the values of the indices.

With these notations, using the description provided in Section IV, the indices of the columns of U corresponding to $\mathcal{T}_{b_\ell, \mu_{b_\ell}}$ may be shown to be

$$2b_s b_i + \mu_{b_\ell} b_s + \{0, \dots, (b_s - 1)\} \quad \text{with} \quad b_i \in \{0, \dots, (b_n - 1)\}. \quad (65)$$

This is more easily interpreted by indexing the stages of the algorithm in the reverse order, thus introducing

$$\widehat{b}_r = b_{\ell m} - b_\ell \quad (66)$$

where $b_{\ell m} = \log_2 d_1$ is the maximum value of b_ℓ and therefore

$$d_1 = 2^{b_{\ell m}}. \quad (67)$$

Using (30), (31), (67) and (66), we obtain

$$b_s = 2^{\widehat{b}_r}. \quad (68)$$

Also using (31), the column indices in (65) may therefore be rewritten as

$$b_i 2^{(b_r+1)} + \mu_{b_\ell} 2^{b_r} + \{0, \dots, (2^{b_r} - 1)\} \quad \text{with } b_i \in \{0, \dots, (2^{b_\ell} - 1)\}. \quad (69)$$

This should be compared to the representation in base 2 of the index of any column of U , that may be expressed as

$$\sum_{j=0}^{b_{\ell m}} c_j 2^j \quad (70)$$

with each bit c_j equal to 0 or 1. Eq. (70) allows one to interpret the set of indices in (69), i.e. the set of indices of the columns of U that correspond to $\mathcal{S}_{b_\ell, m_{b_\ell}} = \mathcal{T}_{b_\ell, \mu_{b_\ell}}$, for given values of m_{b_ℓ} , b_ℓ and hence b_r , due to (66): these column indices are all the indices whose representation in base 2 is such that their bit c_j with index $j = b_r$ is constrained to be equal to μ_{b_ℓ} , whereas all possible combinations are gathered in this set of index values, for all the bits c_j with indices $j \neq b_r$. To summarize, in $\mathcal{S}_{b_\ell, m_{b_\ell}}$, only the bit with index $j = b_r$ of the column index is imposed.

Then, we eventually aim at analyzing the intersections of $(b_{\ell m} + 1)$ subspaces introduced in Section IV. This may be rephrased as follows, using the notations introduced in the present appendix. Each considered intersection of $(b_{\ell m} + 1)$ subspaces $\mathcal{S}_{b_\ell, m_{b_\ell}} = \mathcal{T}_{b_\ell, \mu_{b_\ell}}$ corresponds to one value of the set of indices $\{m_0, \dots, m_{b_{\ell m}}\}$ and therefore $\{\mu_0, \dots, \mu_{b_{\ell m}}\}$. As explained above, separately for each value of b_ℓ and hence of b_r , the columns of U that are kept in this intersection are those whose index represented in base 2 has a bit with index $j = b_r$ that is fixed and equal to μ_{b_ℓ} . The intersection of the complete set of $(b_{\ell m} + 1)$ subspaces obtained when varying b_ℓ thus yields one and only one column of U , namely the one whose bits are all defined by the selected complete set of values $\{\mu_0, \dots, \mu_{b_{\ell m}}\}$. This also entails that, when successively considering the subspace intersections corresponding to all values of $\{\mu_0, \dots, \mu_{b_{\ell m}}\}$, all columns of U are successively obtained. This proves that the proposed method based on subspace intersections is guaranteed to completely identify U (here again up to one phase factor per column, these phase factors being then handled as in the other proposed methods).

The successive subspace intersections may be considered in such an order that the sets of indices $\{\mu_0, \dots, \mu_{b_{\ell m}}\}$ correspond to the representation in base 2 of the integers in increasing order. Then, the columns of U are obtained with indices in increasing order. This is exactly what is obtained in the successive rows of Table 2 in the example provided below.

B. EXAMPLE

We here illustrate the above property and thus the proposed complete multi-stage methods by considering the case $d = 8$, $d_2 = 2$ and hence $d_1 = 4$ and $(\log_2 d_1 + 1) = 3$ stages. During the first stage, that corresponds to $b_\ell = 0$, the eigendecomposition allows one to identify two subspaces \mathcal{S}_{0, m_0} , respectively with $m_0 = 1$ and $m_0 = 2$, and that

respectively correspond to the following sets of 4 indices of columns of U : $\{1, 2, 3, 4\}$ and $\{5, 6, 7, 8\}$. Then, during the second stage, that corresponds to $b_\ell = 1$, the eigen-decomposition allows one to identify two subspaces \mathcal{S}_{1, m_1} , respectively with $m_1 = 1$ and $m_1 = 2$, and that respectively correspond to the following sets of 4 indices of columns of U : $\{1, 2, 5, 6\}$ and $\{3, 4, 7, 8\}$. Finally, the third stage, that corresponds to $b_\ell = 2$, yields the following sets of 4 indices of columns of U : $\{1, 3, 5, 7\}$ and $\{2, 4, 6, 8\}$. We then derive the corresponding subspace intersections, first considering $\mathcal{S}_{0, m_0} \cap \mathcal{S}_{1, m_1}$ as intermediate quantities, and finally deriving $\mathcal{S}_{0, m_0} \cap \mathcal{S}_{1, m_1} \cap \mathcal{S}_{2, m_2}$. All these intersections are listed in Table 2. This proves that the proposed approach yields 8 intersections that are each restricted to one column of U and that this set of intersections yields all the individual columns of U , as required.

C. PSEUDO-CODE

The above analysis also has the advantage of suggesting a possible structure for the software program used to implement this multi-stage QPT method. This program has a recursive structure, combined with a binary tree as follows. It is based on a recursive function, with each call of this function corresponding to one value of the stage index b_ℓ (and hence of b_r) and to one bit of the binary representation (70) of the index of a column of U . In each such call, this function successively considers the two possible values of that bit, that is 0 and 1. For each of them, it determines the intersection of the subspaces with indices 0 to b_ℓ (by determining the subspace with index b_ℓ and combining it with the previously determined intersection of the subspaces with indices 0 to $(b_\ell - 1)$) and it recursively calls itself with this bit value. Successively performing this for each of the two values of the considered bit creates two branches in the tree structure. In each final call of this recursive function, i.e. each leave of the tree, all bits of the column index are assigned, the function determines the corresponding complete subspace intersection and sends it back as one column of the estimate of U . By gathering these columns at each level back from the recursion, the complete matrix that estimates U (up to phase factors at this stage) is obtained.

The corresponding pseudo-code is provided in Algorithm 5 for the main part of the program and Algorithm 6 for the recursive function.

APPENDIX L FLUCTUATION MODEL FOR DENSITY MATRIX ESTIMATION

In Section V, we presented the statistical model that we used in our tests to represent the fluctuations that may be faced when estimating a ket with a QST algorithm. We hereafter describe a corresponding model for the estimation of density matrices. Whereas we eventually apply it to mixed states, we first build it by considering a pure state, to make it compatible with the model used for ket estimation in Section V. We therefore consider a pure state represented by the density

matrix

$$\rho = |\psi\rangle\langle\psi|. \quad (71)$$

Denoting c_k each actual component of $|\psi\rangle$ and ϵ_k the additive random complex-valued error made when estimating it, each actual element of the density matrix ρ reads

$$\rho_{k\ell} = c_k c_\ell^* \quad (72)$$

and its estimated version may be expressed as

$$\hat{\rho}_{k\ell} = (c_k + \epsilon_k)(c_\ell + \epsilon_\ell)^* \quad (73)$$

$$= c_k c_\ell^* + c_k \epsilon_\ell^* + \epsilon_k c_\ell^* + \epsilon_k \epsilon_\ell^*. \quad (74)$$

We aim at building an approximation of that quantity that, as with the “noisy ket model” of Section V, yields a noisy model of the density matrix that is expressed as the sum of the actual density matrix and of a term that represents fluctuations that are consistent with those of the random model used in Section V for kets. To this end, we first note that, in (74), the first term, namely $c_k c_\ell^*$, is nothing but the actual value (72), whereas all other terms are the random fluctuations. We aim at deriving an approximation of these terms, that only depends on 1) the actual value (72), 2) a single random variable ϵ_R for the real part of the fluctuations and 3) a single random variable ϵ_I for the imaginary part of the fluctuations.

As a simple approximation, we separately consider the real and imaginary parts of the fluctuations and then just add them in our final approximate model. The real part is handled as follows. The random variable ϵ_R takes both ϵ_k and ϵ_ℓ of (74) into account. Therefore, it represents an error for a ket component and it is drawn with the same statistics as the fluctuations of a ket component of Section V, i.e. it is real-valued and uniformly drawn over the range $[-w/2, w/2]$. In other words, to obtain a simple model, both ϵ_k and ϵ_ℓ are here replaced by ϵ_R in (74) (without taking their possible statistical independence into account). Then, to express this real-valued part of the fluctuation model only with respect to $\rho_{k\ell}$ in addition to ϵ_R , as explained above, we ignore the phases of c_k and c_ℓ^* in the second and third terms of (74) and we replace both of them with $\sqrt{|\rho_{k\ell}|}$, based on (72). The resulting approximate model for the real part of fluctuations, corresponding to the real part of the last three terms of (74), is thus equal to $2\sqrt{|\rho_{k\ell}|}\epsilon_R + \epsilon_R^2$.

As explained above, the imaginary part of fluctuations is handled in the same way and just added to the above real part. As an overall result, the complete approximate noisy model for any density matrix element reads

$$\hat{\rho}_{k\ell} = \rho_{k\ell} + 2\sqrt{|\rho_{k\ell}|}\epsilon_R + \epsilon_R^2 + i(2\sqrt{|\rho_{k\ell}|}\epsilon_I + \epsilon_I^2). \quad (75)$$

We again stress that this model contains approximations but meets the required constraints: it allows one to create a “noisy” version $\hat{\rho}_{k\ell}$ of a given “noiseless” density matrix element $\rho_{k\ell}$ by just drawing a sample of each of the random variables ϵ_R and ϵ_I , whose statistics are defined in a way which is qualitatively consistent with those of the random

variable used in Section V for deriving a “noisy” version of a ket component. This then mainly allows us to compare the performance of several QPT methods with the same (relevant) fluctuation statistics. This qualitative relevance of our simplified model is thus sufficient for our needs. This is to be contrasted with, e.g., the situation when one would consider a given physical system and one would have to develop a model of it that is as accurate as possible.

REFERENCES

- [1] M. A. Nielsen and I. L. Chuang, *Quantum computation and quantum information*. Cambridge, UK: Cambridge University Press, 2000.
- [2] I. L. Chuang and M. A. Nielsen, “Prescription for experimental determination of the dynamics of a quantum black box,” *Journal of Modern Optics*, vol. 44, no. 11-12, pp. 2455–2467, 1997.
- [3] C. H. Baldwin, A. Kalev, and I. Deutsch, “Quantum process tomography of unitary and near-unitary maps,” *Physical Review A*, vol. 90, pp. 012 110–1 to 012 110–10, 2014.
- [4] R. Blume-Kohout, J. K. Gamble, E. Nielsen, J. Mizrahi, J. D. Sterk, and P. Maunz, “Robust, self-consistent, closed-form tomography of quantum logic gates on a trapped ion qubit,” *arXiv:1310.4492v1*, 16 Oct. 2013.
- [5] M. P. A. Branderhorst, J. Nunn, I. A. Walmsley, and R. L. Kosut, “Simplified quantum process tomography,” *New Journal of Physics*, vol. 11, pp. 115 010+12, 2009.
- [6] S. T. Merkel, J. M. Gambetta, J. A. Smolin, S. Poletto, A. D. Córcoles, B. R. Johnson, C. A. Ryan, and M. Steffen, “Self-consistent quantum process tomography,” *Physical Review A*, vol. 87, pp. 062 119–1 to 062 119–9, 2013.
- [7] N. Navon, N. Akerman, S. Kotler, Y. Glickman, and R. Ozeri, “Quantum process tomography of a Mølmer-Sørensen interaction,” *Physical Review A*, vol. 90, pp. 010 103–1 to 010 103–5, 2014.
- [8] A. Shukla and T. S. Mahesh, “Single-scan quantum process tomography,” *Physical Review A*, vol. 90, pp. 052 301–1 to 052 301–6, 2014.
- [9] M. Takahashi, S. D. Bartlett, and A. C. Doherty, “Tomography of a spin qubit in a double quantum dot,” *Physical Review A*, vol. 88, pp. 022 120–1 to 022 120–9, 2013.
- [10] Y. Wang, D. Dong, I. R. Petersen, and J. Zhang, “An approximate algorithm for quantum Hamiltonian identification with complexity analysis,” in *Proceedings of the 20th World Congress of the International Federation of Automatic Control (IFAC 2017)*, Toulouse, France, July 9–14 2017, pp. 12 241–12 245.
- [11] A. G. White and A. Gilchrist, “Measuring two-qubit gates,” *Journal of the Optical Society of America B*, vol. 24, no. 2, pp. 172–183, Feb. 2007.
- [12] A. Shabani, R. L. Kosut, M. Mohseni, H. Rabitz, M. A. Broome, M. P. Almeida, A. Fedrizzi, and A. G. White, “Efficient measurement of quantum dynamics via compressive sensing,” *Physical Review Letters*, vol. 106, no. 10 (Mar.), p. 100401 (4 pages), 2011.
- [13] S. Kimmel and Y. K. Liu, “Phase retrieval using unitary 2-designs,” in *2017 International Conference on Sampling Theory and Applications (SampTA)*, Tallinn, Estonia, July (03–07) 2017, pp. 345–349.
- [14] J. Fiurásek and Z. Hradil, “Maximum-likelihood estimation of quantum processes,” *Physical Review A*, vol. 63, no. 2, p. 020101 (4 pages), 2001.
- [15] H. Sakhouf, M. Daoud, and R. Ahl-Laamara, “Quantum process tomography of the single-shot entangling gate with superconducting qubits,” *Journal of Physics B: Atomic, Molecular and Optical Physics*, vol. 56, no. 10, p. 105501, 2023.
- [16] S. Xiao, Y. Wang, D. Dong, and J. Zhang, “Two-stage solution for ancilla-assisted quantum process tomography: Error analysis and optimal design,” in *2023 62nd IEEE Conference on Decision and Control (CDC)*, 2023, pp. 7178–7183.
- [17] S.G. Stanchev and N. Vitanov, “Multipass quantum process tomography,” *Scientific Reports*, vol. 14, p. paper no. 18185, 2024.
- [18] S. Xiao, Y. Wang, J. Zhang, D. Dong, G.-J. Mooney, I.-R. Petersen, and H. Yonezawa, “A two-stage solution to quantum process tomography: error analysis and optimal design,” *IEEE Transactions on Information Theory*, vol. 71, no. 3, pp. 1803–1823, 2025.
- [19] M. Antesberger, M. T. Quintino, P. Walther, and L. A. Rozema, “Higher-order process matrix tomography of a passively-stable quantum switch,” *PRX Quantum*, vol. 5, no. 1, p. paper no. 010325 (22 pages), 2024.

[20] D. Dobrynin, L. Cardarelli, M. Muller, and A. Bermudez, “Compressed-sensing lindbladian quantum tomography with trapped ions,” 2024. [Online]. Available: <https://arxiv.org/abs/2403.07462>

[21] S. Xue, G. Huang, Y. Liu, D. Wang, W. Shi, Y. Liu, X. Fu, A. Huang, M. Deng, and J. Wu, “Efficient quantum process tomography for Clifford circuits,” *Physical Review A*, vol. 108, no. 3, p. paper no. 032419 (9 pages), 2023.

[22] F. Verdeil and Y. Deville, “Unitary quantum process tomography with unreliable pure input states,” *Physical Review A*, vol. 108, no. 6, p. 062410 (20 pages), 2023.

[23] S. Xue, Y. Liu, Y. Wang, P. Zhu, C. Guo, and J. Wu, “Variational quantum process tomography of unitaries,” *Physical Review A*, vol. 105, no. 3, p. 032427 (8 pages), 2022.

[24] G. Gutoski and N. Johnston, “Process tomography for unitary quantum channels,” *Journal of Mathematical Physics*, vol. 55, no. 3, p. 032201 (19 pages), 2014.

[25] I. Lopez Gutierrez, F. Dietrich, and C. Mendl, “Quantum process tomography of unitary maps from time-delayed measurements,” *Quantum Information Processing*, vol. 22, p. paper no. 251, 2023.

[26] J. Escandón-Monardes, D. Uzcátegui, M. Rivera-Tapia, S. Walborn, and A. Delgado, “Estimation of high-dimensional unitary transformations saturating the Quantum Cramér-Rao bound,” *Quantum*, vol. 8, p. 1405, 2024.

[27] H. Zhao, L. Lewis, I. Kannan, Y. Quek, H.-Y. Huang, and M. Caro, “Learning quantum states and unitaries of bounded gate complexity,” *PRX Quantum*, vol. 5, no. 4, p. 040306, 2024.

[28] IBM, “Bringing useful quantum computing to the world,” <https://www.ibm.com/quantum>, accessed on line on Nov. 22, 2024.

[29] —, “Qiskit,” <https://www.ibm.com/quantum/qiskit>, accessed on line on Nov. 22, 2024.

[30] —, “Circuit library,” <https://docs.quantum.ibm.com/guides/circuit-library>, accessed on line on Nov. 22, 2024.

[31] —, “Circuit library / standard gates,” https://docs.quantum.ibm.com/api/qiskit/circuit_library#standard-gates, accessed on line on Nov. 22, 2024.

[32] Amazon, “Amazon braket terms and concepts,” <https://docs.aws.amazon.com/braket/latest/developerguide/braket-terms.html>, accessed on line on Nov. 22, 2024.

[33] Mathworks, “Introduction to quantum computing,” <https://fr.mathworks.com/help/matlab/math/introduction-to-quantum-computing.html>, accessed on line on Nov. 22, 2024.

[34] T. Odake, S. Yoshida, and M. Murao, “Analytical lower bound on the number of queries to a black-box unitary operation in deterministic exact transformations of unknown unitary operations,” 2024. [Online]. Available: <https://arxiv.org/abs/2405.07625>

[35] Y. Deville, L. T. Duarte, and A. Deville, “A taxonomy of relationships between information processing, machine learning and quantum physics: quantum-inspired, quantum-assisted, quantum-targeted and related approaches,” in *Proceedings of the 2024 IEEE Mediterranean and Middle-East Geoscience and Remote Sensing Symposium (M2GARSS 2024)*, Oran, Algeria, April (15-17) 2024, pp. 361–365.

[36] Y. Deville and A. Deville, “New single-preparation methods for unsupervised quantum machine learning problems,” *IEEE Transactions on Quantum Engineering*, vol. 2, no. Article Sequence Number: 3104224, DOI: 10.1109/TQE.2021.3121797, pp. 1–24, 2021.

[37] —, “From blind quantum source separation to blind quantum process tomography,” in *Proceedings of the 12th International Conference on Latent Variable Analysis and Signal Separation (LVA/ICA 2015)*, Liberec, Czech Republic, Springer International Publishing Switzerland, LNCS 9237, Aug. 25-28 2015, pp. 184–192.

[38] —, “The blind version of quantum process tomography: operating with unknown input values,” in *Proceedings of the 20th World Congress of the International Federation of Automatic Control (IFAC 2017)*, Toulouse, France, July 9-14 2017, pp. 12 228–12 234.

[39] —, “Quantum process tomography with unknown single-preparation input states: Concepts and application to the qubit pair with internal exchange coupling,” *Physical Review A*, vol. 101, no. 4, pp. 042 332–1 to 042 332–18, April 2020.

[40] —, “Blind separation of quantum states: estimating two qubits from an isotropic Heisenberg spin coupling model,” in *Proceedings of the 7th International Conference on Independent Component Analysis and Signal Separation (ICA 2007)*, ISSN 0302-9743, Springer-Verlag, vol. LNCS 4666. *Erratum: replace two terms $E\{r_i\}E\{q_i\}$ in (33) of [40]* by $E\{r_iq_i\}$, since q_i depends on r_i ., London, UK, Sept. 9-12 2007, pp. 706–713.

[41] —, “Exploiting the higher-order statistics of random-coefficient pure states for quantum information processing,” *Quantum Information Processing*, vol. 22, no. 216 (Article number), 2023.

[42] Mathworks, “Sparse matrices,” <https://www.mathworks.com/help/matlab/sparse-matrices.html>, accessed on line on June 25, 2024.

[43] A. Shabani, M. Mohseni, S. Lloyd, R. L. Kosut, and H. Rabitz, “Estimation of many-body quantum Hamiltonians via compressive sensing,” *Physical Review A*, vol. 84, no. 1 (Jul.), p. 012107 (8 pages), 2011.

[44] D. M. Reich, G. Gualdi, and C. P. Koch, “Minimum number of input states required for quantum gate characterization,” *Physical Review A*, vol. 88, no. 4, p. 042309 (paper no.; 9 pages), 2013.

[45] A. Messiah, *Mécanique quantique - 1*. Paris: Dunod, 1962.

[46] R. P. Feynman, *Statistical mechanics. A set of lectures*. Reading (Massachusetts): W. A. Benjamin Inc., 1972.

[47] U. Fano, “Description of states in quantum mechanics by density matrix and operator techniques,” *Reviews of Modern Physics*, vol. 29, no. 1 (Jan.), pp. 74–93, 1957.

[48] R. A. Horn and C. R. Johnson, *Matrix analysis*. Cambridge, United Kingdom: Cambridge University Press, 1985.

[49] —, *Matrix analysis*. Cambridge, United Kingdom: Cambridge University Press, 2013.

[50] A. Hyvärinen, J. Karhunen, and E. Oja, *Independent Component Analysis*. New York: Wiley, 2001.

[51] A. Papoulis, *Probability, random variables, and stochastic processes*. Singapore: McGraw-Hill, 1984.

[52] L. L. Scharf, *Statistical signal processing. Detection, estimation and time series analysis*. Reading, Massachusetts: Addison-Wesley, 1991.

[53] A. Smilde, R. Bro, and P. Geladi, *Multi-way analysis with applications in the chemical sciences*. Chichester, England: Wiley, 2004.

[54] G. Saporta, *Probabilités, Analyse des données et statistique*. Paris: Technip, 1990.

[55] Mathworks, “Canonical correlation analysis,” <https://fr.mathworks.com/help/stats/canoncorr.html>, accessed on line on March 4, 2024.

[56] A. Boulais, Y. Deville, and O. Berné, “A blind identification and source separation method based on subspace intersections for hyperspectral astrophysical data,” in *13th International Conference on Latent Variable Analysis and Signal Separation (LVA/ICA 2017)*, Grenoble, France (Springer International Publishing AG 2017, LNCS 10169), Feb. 21-23 2017, pp. 367–380.

[57] Y. Deville, L. T. Duarte, and S. Hosseini, *Nonlinear blind source separation and blind mixture identification. Methods for bilinear, linear-quadratic and polynomial mixtures*. Springer Nature (SpringerBriefs in Electrical and Computer Engineering), 2021.

[58] Y. Deville, *Wiley Encyclopedia of Electrical and Electronics Engineering*. Wiley, J. Webster (ed.), 2016, ch. Blind source separation and blind mixture identification methods, pp. 1–33.

[59] L. DeLathauwer, J. Castaing, and J.-F. Cardoso, “Fourth-order cumulant-based blind identification of underdetermined mixtures,” *IEEE Transactions on Signal Processing*, vol. 55, no. 6, pp. 2965–2973, 2007.

[60] L. Tong, R. Liu, V. C. Soon, and Y.-F. Huang, “Indeterminacy and identifiability of blind identification,” *IEEE Transactions on Circuits and Systems*, vol. 38, no. 5, pp. 499–509, 1991.

[61] A. I. Lvovsky and M. G. Raymer, “Continuous-variable optical quantum-state tomography,” *Reviews of Modern Physics*, vol. 81, no. 1, pp. 299–332, 2009.

[62] J. Medford, J. Beil, J. M. Taylor, S. D. Bartlett, A. C. Doherty, E. I. Rashba, D. P. DiVincenzo, H. Lu, A. C. Gossard, and C. M. Marcus, “Self-consistent measurement and state tomography of an exchange-only spin qubit,” *Nature Nanotechnology*, vol. 8, no. Sept., pp. 654–659, 2013.

[63] C. Stark, “Self-consistent tomography of the state-measurement gram matrix,” *Physical Review A*, vol. 89, pp. 052 109–1 to 052 109–8, 2014.

[64] D. F. V. James, P. G. Kwiat, W. J. Munro, and A. G. White, “Measurement of qubits,” *Physical Review A*, vol. 64, p. 052312 (15 pages), 2001.

[65] I. Roth, J. Wilkens, D. Hangleiter, and J. Eisert, “Semi-device-dependent blind quantum tomography,” *Quantum*, vol. 7, no. Jul., p. 1053, 2023.

[66] A. Melkani, C. Gneiting, and F. Nori, “Eigenstate extraction with neural-network tomography,” *Physical Review A*, vol. 102, no. 2, pp. 022 412–1 to 022 412–11, 2020.

[67] S. Ahmed, C. S. Munoz, F. Nori, and A. F. Kockum, “Quantum state tomography with conditional generative adversarial networks,” *Physical Review Letters*, vol. 127, no. 14 (Sep.), p. 140502 (8 pages), 2021.

[68] ——, “Classification and reconstruction of optical quantum states with deep neural networks,” *Physical Review Research*, vol. 3, no. 3 (Sep.), p. 033278 (36 pages), 2021.

[69] J. Altepeter, E. Jeffrey, and P. Kwiat, “Photonic state tomography,” *Advances In Atomic, Molecular, and Optical Physics*, vol. 52, pp. 105–159, 2005.

[70] S. T. Flammia, D. Gross, Y.-K. Liu, and J. Eisert, “Quantum tomography via compressed sensing: error bounds, sample complexity and efficient estimators,” *New Journal of Physics*, vol. 14, p. 095022 (28 pages), 2012.

[71] D. Dong, Y. Wang, Z. Hou, B. Qi, Y. Pan, and G.-Y. Xiang, “State tomography of qubit systems using linear regression estimation and adaptive measurements,” in *Proceedings of the 20th World Congress of the International Federation of Automatic Control (IFAC 2017)*, Toulouse, France, July 9-14 2017, pp. 13 556–13 561.

[72] M. K. Kurmapu, V. V. Tiunova, E. S. Tiunov, M. Ringbauer, C. Maier, R. Blatt, T. Monz, A. K. Fedorov, and A. Lvovsky, “Reconstructing complex states of a 20-qubit quantum simulator,” *PRX Quantum*, vol. 4, no. 4, p. 040345 (paper no.; 9 pages), 2023.

[73] R. Stricker, M. Meth, L. Postler, C. Edmunds, C. Ferrie, R. Blatt, P. Schindler, T. Monz, R. Kueng, and M. Ringbauer, “Experimental single-setting quantum state tomography,” *PRX Quantum*, vol. 3, p. 040310 (34 pages), 2022.

[74] G. H. Golub and C. F. V. Loan, *Matrix computations*. Baltimore: Johns Hopkins University Press, 1996.

[75] Mathworks, “QR decomposition,” <https://fr.mathworks.com/help/matlab/ref/qr.html>, accessed on line on May 22, 2025.

[76] A. Cichocki and S.-I. Amari, *Adaptive blind signal and image processing. Learning algorithms and applications*. Chichester, England: Wiley, 2002.

[77] P. Comon and C. Jutten, *Handbook of blind source separation. Independent component analysis and applications*. Oxford, UK: Academic Press, 2010.

[78] S. Makino, T.-W. Lee, and H. S. (Eds), *Blind speech separation*. Dordrecht, The Netherlands: Springer, 2007.

[79] A. Belouchrani, K. Abed-Meraim, J.-F. Cardoso, and E. Moulines, “A blind source separation technique using second-order statistics,” *IEEE Transactions on Signal Processing*, vol. 45, no. 2, pp. 434–444, 1997.

[80] L. Fety, *Méthodes de traitement d’antenne adaptées aux radiocommunications*. Paris (France): Thèse ENST, 1988.

[81] S. Hosseini, Y. Deville, and H. Saylani, “Blind separation of linear instantaneous mixtures of non-stationary signals in the frequency domain,” *Signal Processing*, vol. 89, no. 5, pp. 819–830, 2009.

[82] L. Molgedey and H. Schuster, “Separation of a mixture of independent signals using time delayed correlation,” *Physical Review Letters*, vol. 72, no. 23, pp. 3634–3637, 1994.

[83] J. von Neumann, *Mathematical foundations of quantum mechanics* (translated from the German edition). Princeton: Princeton University Press, 1955.

[84] A. Peres, *Quantum theory: concepts and methods*. Dordrecht, The Netherlands: Kluwer Academic, 1995.

...

Input : a) Estimate $\hat{\rho}_4$ of output density matrix ρ_2 (provided by QST and obtained for input density matrix (17) with the diagonal values defined in (19)). b) Estimate $\hat{\rho}_8$ of output density matrix ρ_6 (provided by QST and obtained for input density matrix (21) with the diagonal values defined in (19)).
 c) Estimate $|\hat{\Psi}_2\rangle$ of output ket $|\Psi_2\rangle$ (provided by QST and obtained for all components of input ket $|\Psi_1\rangle$ equal to $1/\sqrt{d}$).

Output: Estimate \hat{U}_5 of quantum process matrix U .

begin

/* Exploit $\hat{\rho}_4$: */
 Eigendecomposition: derive 1) a diagonal matrix D_4 that contains the eigenvalues of $\hat{\rho}_4$ in an arbitrary order and 2) a matrix V_4 whose columns are eigenvectors of $\hat{\rho}_4$ in the same order as eigenvalues;
 Reorder the eigenvalues in D_4 in nonincreasing order and apply the same permutation to the columns of V_4 to create the matrix \hat{U}_2 ;
 /* Exploit $\hat{\rho}_8$: */
 Eigendecomposition: derive 1) a diagonal matrix D_8 that contains the eigenvalues of $\hat{\rho}_8$ in an arbitrary order and 2) a matrix V_8 whose columns are eigenvectors of $\hat{\rho}_8$ in the same order as eigenvalues;
 Reorder the eigenvalues in D_8 in nonincreasing order and apply the same permutation to the columns of V_8 to create the matrix \hat{U}_3 ;
 /* Combine \hat{U}_2 and \hat{U}_3 : */
for $m_1 = 1$ to d_2 **do**
for $m_2 = 1$ to d_2 **do**
 Set column of \hat{U}_4 with index equal to $((m_1 - 1)d_1 + m_2)$: Set it to first vector provided by CCA of 1) the set of columns of \hat{U}_2 with indices $((m_1 - 1)d_1 + n_1)$ with $n_1 \in \{1, \dots, d_1\}$ and 2) the set of columns of \hat{U}_3 with indices $((m_2 - 1)d_1 + n_2)$ with $n_2 \in \{1, \dots, d_1\}$;
 /* If the CCA tool does not provide unit-norm vectors, then do it: */
 Divide above column of \hat{U}_4 by its norm;
end
end
 /* Exploit $|\hat{\Psi}_2\rangle$: */
 $|\Psi_3\rangle = \hat{U}_4^\dagger |\hat{\Psi}_2\rangle$;
 $\hat{U}_5 = \hat{U}_4 \text{ diag}(|\Psi_3\rangle \otimes |\Psi_1\rangle)$;

end

Algorithm 2: EQPT2: second Eigenanalysis-based QPT algorithm (composed of two stages). This version is for the case when the QST algorithm provides estimates that meet the known properties of the actual quantities. Otherwise, see text.

Method	number of qubits												
	1	2	3	4	5	6	7	8	9	10	11	12	13
EQPT1	$\simeq 1$ ms	$\simeq 1$ ms	$\simeq 1$ ms	$\simeq 1$ ms	2.2 ms	3.9 ms	7.2 ms	22 ms	68 ms	400 ms	3.1 s	23 s	170 s
EQPT2				2.6 ms		15 ms		170 ms		4.3 s		180 s	
EQPT3				2.8 ms		18 ms		200 ms		5.0 s		230 s	
EQPT5			2.3 ms	5.4 ms	27 ms	100 ms	580 ms	4.4 s	38 s	490 s $\simeq 8$ mn	7600 s $\simeq 2$ h 07 mn		

TABLE 1. Execution times (averaged over tests with all values of w) of the EQPT1, EQPT2, EQPT3 and EQPT5 methods vs. number of qubits.

Input : a) Estimate $\hat{\rho}_4$ of output density matrix ρ_2 (provided by QST and obtained for input density matrix (17) with the diagonal values defined in (19)). b) Estimate $\hat{\rho}_8$ of output density matrix ρ_6 (provided by QST and obtained for input density matrix (21) with the diagonal values defined in (19)). c) Estimate $|\hat{\Psi}_2\rangle$ of output ket $|\Psi_2\rangle$ (provided by QST and obtained for all components of input ket $|\Psi_1\rangle$ equal to $1/\sqrt{d}$).

Output: Estimate \hat{U}_5 of quantum process matrix U .

begin

```
/* Exploit  $\hat{\rho}_4$ : */  
Eigendecomposition: derive 1) a diagonal matrix  $D_4$  that contains the eigenvalues of  $\hat{\rho}_4$  in an arbitrary order and 2) a matrix  $V_4$  whose columns are eigenvectors of  $\hat{\rho}_4$  in the same order as eigenvalues; Reorder the eigenvalues in  $D_4$  in nonincreasing order and apply the same permutation to the columns of  $V_4$  to create the matrix  $\hat{U}_2$ ;  
/* Exploit  $\hat{\rho}_8$ : */  
Eigendecomposition: derive 1) a diagonal matrix  $D_8$  that contains the eigenvalues of  $\hat{\rho}_8$  in an arbitrary order and 2) a matrix  $V_8$  whose columns are eigenvectors of  $\hat{\rho}_8$  in the same order as eigenvalues; Reorder the eigenvalues in  $D_8$  in nonincreasing order and apply the same permutation to the columns of  $V_8$  to create the matrix  $\hat{U}_3$ ;  
/* Combine  $\hat{U}_2$  and  $\hat{U}_3$ : */  
for  $m_1 = 1$  to  $d_2$  do  
  for  $m_2 = 1$  to  $d_2$  do  
    Set column of  $\hat{U}_4$  with index equal to  $((m_1 - 1)d_1 + m_2)$ : Set it to first vector provided by CCA of 1) the set of columns of  $\hat{U}_2$  with indices  $((m_1 - 1)d_1 + n_1)$  with  $n_1 \in \{1, \dots, d_1\}$  and 2) the set of columns of  $\hat{U}_3$  with indices  $((m_2 - 1)d_1 + n_2)$  with  $n_2 \in \{1, \dots, d_1\}$ ;  
    /* If the CCA tool does not provide unit-norm vectors, then do it: */  
    Divide above column of  $\hat{U}_4$  by its norm;  
  end  
end  
Find decomposition of  $\hat{U}_4$  as  $\hat{U}_4 = V\Sigma W^\dagger$  with SVD;  
 $\hat{U}_{4u} = VW^\dagger$ ;  
/* Exploit  $|\hat{\Psi}_2\rangle$ : */  
 $|\Psi_3\rangle = \hat{U}_{4u}^\dagger |\hat{\Psi}_2\rangle$ ;  
 $\hat{U}_5 = \hat{U}_{4u} \text{ diag}(|\Psi_3\rangle \otimes |\Psi_1\rangle)$ ;
```

end

Algorithm 3: EQPT3: third Eigenanalysis-based QPT algorithm (composed of two stages). This version is for the case when the QST algorithm provides estimates that meet the known properties of the actual quantities. Otherwise, see text.

Input : a) Estimate $\hat{\rho}_4$ of output density matrix ρ_2 (provided by QST and obtained for input density matrix (17) with the diagonal values defined in (19)). b) Estimate $\hat{\rho}_8$ of output density matrix ρ_6 (provided by QST and obtained for input density matrix (21) with the diagonal values defined in (19)). c) Estimate $|\hat{\Psi}_2\rangle$ of output ket $|\Psi_2\rangle$ (provided by QST and obtained for all components of input ket $|\Psi_1\rangle$ equal to $1/\sqrt{d}$).

Output: Estimate \hat{U}_5 of quantum process matrix U .

begin

```
/* Exploit  $\hat{\rho}_4$ : */  
Eigendecomposition: derive 1) a diagonal matrix  $D_4$  that contains the eigenvalues of  $\hat{\rho}_4$  in an arbitrary order and 2) a matrix  $V_4$  whose columns are eigenvectors of  $\hat{\rho}_4$  in the same order as eigenvalues; Reorder the eigenvalues in  $D_4$  in nonincreasing order and apply the same permutation to the columns of  $V_4$  to create the matrix  $\hat{U}_2$ ;  
/* Exploit  $\hat{\rho}_8$ : */  
Eigendecomposition: derive 1) a diagonal matrix  $D_8$  that contains the eigenvalues of  $\hat{\rho}_8$  in an arbitrary order and 2) a matrix  $V_8$  whose columns are eigenvectors of  $\hat{\rho}_8$  in the same order as eigenvalues; Reorder the eigenvalues in  $D_8$  in nonincreasing order and apply the same permutation to the columns of  $V_8$  to create the matrix  $\hat{U}_3$ ;  
/* Combine  $\hat{U}_2$  and  $\hat{U}_3$ : */  
for  $m_1 = 1$  to  $d_2$  do  
  for  $m_2 = 1$  to  $d_2$  do  
    Set column of  $\hat{U}_4$  with index equal to  $((m_1 - 1)d_1 + m_2)$ : Set it to first vector provided by CCA of 1) the set of columns of  $\hat{U}_2$  with indices  $((m_1 - 1)d_1 + n_1)$  with  $n_1 \in \{1, \dots, d_1\}$  and 2) the set of columns of  $\hat{U}_3$  with indices  $((m_2 - 1)d_1 + n_2)$  with  $n_2 \in \{1, \dots, d_1\}$ ;  
    /* If the CCA tool does not provide unit-norm vectors, then do it: */  
    Divide above column of  $\hat{U}_4$  by its norm;  
  end  
end  
/* Exploit  $|\hat{\Psi}_2\rangle$ : */  
 $|\Psi_3\rangle = \hat{U}_4^\dagger |\hat{\Psi}_2\rangle$ ;  
 $\hat{U}_{5p} = \hat{U}_4 \text{ diag}(|\Psi_3\rangle \otimes |\Psi_1\rangle)$ ;  
Find decomposition of  $\hat{U}_{5p}$  as  $\hat{U}_{5p} = V\Sigma W^\dagger$  with SVD;  
 $\hat{U}_5 = VW^\dagger$ ;
```

end

Algorithm 4: EQPT4: fourth Eigenanalysis-based QPT algorithm (composed of two stages). This version is for the case when the QST algorithm provides estimates that meet the known properties of the actual quantities. Otherwise, see text.

\mathcal{S}_{0,m_0}	\mathcal{S}_{1,m_1}	\mathcal{S}_{2,m_2}	$\mathcal{S}_{0,m_0} \cap \mathcal{S}_{1,m_1}$	$\mathcal{S}_{0,m_0} \cap \mathcal{S}_{1,m_1} \cap \mathcal{S}_{2,m_2}$
$\{1, 2, 3, 4\}$	$\{1, 2, 5, 6\}$	$\{1, 3, 5, 7\}$	$\{1, 2\}$	$\{1\}$
$\{1, 2, 3, 4\}$	$\{1, 2, 5, 6\}$	$\{2, 4, 6, 8\}$	$\{1, 2\}$	$\{2\}$
$\{1, 2, 3, 4\}$	$\{3, 4, 7, 8\}$	$\{1, 3, 5, 7\}$	$\{3, 4\}$	$\{3\}$
$\{1, 2, 3, 4\}$	$\{3, 4, 7, 8\}$	$\{2, 4, 6, 8\}$	$\{3, 4\}$	$\{4\}$
$\{5, 6, 7, 8\}$	$\{1, 2, 5, 6\}$	$\{1, 3, 5, 7\}$	$\{5, 6\}$	$\{5\}$
$\{5, 6, 7, 8\}$	$\{1, 2, 5, 6\}$	$\{2, 4, 6, 8\}$	$\{5, 6\}$	$\{6\}$
$\{5, 6, 7, 8\}$	$\{3, 4, 7, 8\}$	$\{1, 3, 5, 7\}$	$\{7, 8\}$	$\{7\}$
$\{5, 6, 7, 8\}$	$\{3, 4, 7, 8\}$	$\{2, 4, 6, 8\}$	$\{7, 8\}$	$\{8\}$

TABLE 2. Multi-stage QPT method. Each column of the table contains the indices of the column vectors that correspond to the considered subspace or subspace intersection defined in the first row of the table.

Input : a) Set $\{\hat{\rho}_{out,b_\ell}\}$ of estimates of output density matrices of process (provided by QST and obtained for input density matrices defined in Section IV): one estimate for each stage b_ℓ of recursion in Algorithm 6,
 b) Estimate $|\hat{\Psi}_2\rangle$ of output ket $|\Psi_2\rangle$ (provided by QST and obtained for all components of input ket $|\Psi_1\rangle$ equal to $1/\sqrt{d}$).

Output: Estimate \hat{U}_5 of quantum process matrix U .

```

begin
  /* Exploit  $\{\hat{\rho}_{out,b_\ell}\}$ : */  

   $\hat{U}_2 = \text{EQPT5-sub}(0, \{\hat{\rho}_{out,b_\ell}\}, 0);$   

  /* Exploit  $|\hat{\Psi}_2\rangle$ : */  

   $|\Psi_3\rangle = \hat{U}_2^\dagger |\hat{\Psi}_2\rangle;$   

   $\hat{U}_5 = \hat{U}_2 \text{ diag}(|\Psi_3\rangle \otimes |\Psi_1\rangle);$ 
end

```

Algorithm 5: EQPT5-main: main part of fifth Eigenanalysis-based QPT algorithm (composed of multiple stages). This version is for the case when the QST algorithm provides estimates that meet the known properties of the actual quantities. Otherwise, see text.

Input : a) Index b_ℓ of recursion stage, b) Set $\{\hat{\rho}_{out,b_\ell}\}$ of estimates of output density matrices of process (see Algorithm 5), c) Matrix \mathcal{I} whose column vectors form a basis of subspace intersection determined in previous stages of recursion (none in first stage).

Output: matrix \hat{U}_{part} related to estimation of part of quantum process matrix U .

begin

/* Set auxiliary variables (using d : state space dimension; $d_1 = d/2$) :

*/

$b_{\ell m} = \log_2 d_1$;

$b_n = 2^{b_\ell}$;

$b_s = d_1/b_n$;

/* Exploit single estimated output density matrix $\hat{\rho}_{out,b_\ell}$ corresponding to current stage b_ℓ of recursion:

*/

Eigendecomposition: derive 1) a diagonal matrix D_4 that contains the eigenvalues of $\hat{\rho}_{out,b_\ell}$ in an arbitrary order and 2) a matrix V_4 whose columns are eigenvectors of $\hat{\rho}_{out,b_\ell}$ in the same order as eigenvalues;

Reorder the eigenvalues in D_4 in nonincreasing order and apply the same permutation to the columns of V_4 to create the matrix \hat{U}_{b_ℓ} ;

Store the first d_1 columns and last d_1 columns of \hat{U}_{b_ℓ} respectively in matrices $\hat{U}_{b_\ell}(1)$ and $\hat{U}_{b_\ell}(2)$;

/* Derive intersections $\mathcal{I}(1)$ and $\mathcal{I}(2)$ of subspaces defined by $\hat{U}_{b_\ell}(1)$ and $\hat{U}_{b_\ell}(2)$ with subspace defined by \mathcal{I} (if any) :

*/

if $b_\ell = 0$ **then**

$\mathcal{I}(1) = \hat{U}_{b_\ell}(1)$;

$\mathcal{I}(2) = \hat{U}_{b_\ell}(2)$;

end

else

$\mathcal{I}(1) =$ first b_s column vectors provided by CCA of \mathcal{I} and $\hat{U}_{b_\ell}(1)$;

$\mathcal{I}(2) =$ first b_s column vectors provided by CCA of \mathcal{I} and $\hat{U}_{b_\ell}(2)$;

end

if $b_\ell < b_{\ell m}$ **then**

$\hat{U}_{part}(1) =$ EQPT5-sub $(b_\ell + 1, \{\hat{\rho}_{out,b_\ell}\}, \mathcal{I}(1))$;

$\hat{U}_{part}(2) =$ EQPT5-sub $(b_\ell + 1, \{\hat{\rho}_{out,b_\ell}\}, \mathcal{I}(2))$;

end

else

 /* If the CCA tool does not provide unit-norm vectors, then do it: */

$\hat{U}_{part}(1) = \mathcal{I}(1)/\text{norm}(\mathcal{I}(1))$;

$\hat{U}_{part}(2) = \mathcal{I}(2)/\text{norm}(\mathcal{I}(2))$;

end

$\hat{U}_{part} =$ concatenation of columns of $\hat{U}_{part}(1)$ and $\hat{U}_{part}(2)$;

end

Algorithm 6: EQPT5-sub: recursively called sub-program of fifth Eigenanalysis-based QPT algorithm (composed of multiple stages). This version is for the case when the QST algorithm provides estimates that meet the known properties of the actual quantities. Otherwise, see text.